EVALUATION OF THE ES-2 DUMMY IN REPRESENTATIVE SIDE IMPACTS

Randa Radwan Samaha, Matthew R. Maltese
National Highway Traffic Safety Administration
John Bolte
Transportation Research Center
486

ABSTRACT

An upgrade of EUROSID-1, the side impact dummy used in the European Union Side Impact Directive 96/EC/27, was recently developed by TNO to address dummy response issues raised by industrial and governmental bodies, in particular, the flat-top anomaly in the rib deflections. NHTSA is evaluating the ES-2 dummy, the upgraded EUROSID-1, to assess its performance in the FMVSS 214 test configuration. This paper presents results from NHTSA's testing of the ES-2 including high mass pendulum impactor tests using three proposed rib designs, biofidelity sled tests comparing the ES-2 and U.S. SID, and full scale side impact tests.

INTRODUCTION

In 1997, based on NHTSA's side impact harmonization plan submitted to the US Congress [1], the agency performed a series of research crash tests of FMVSS 214 compliant vehicles using the EU 96/EC/27 test procedure and the EUROSID-1 dummy [2]. A main finding from the tests was that plateaus, termed "flat-top" behavior, were present in the dummy rib deflections for all the tests. Rib deflection flat tops are of concern, especially at low levels of deflection, as they are an indication that the rib deflection mechanism is binding and thus the thorax is not responding correctly to the load from the intruding side structure. Thus, the resulting rib deflections and the V*C computations which are based on the rib deflection would be suspect. To further research the flat top phenomenon, NHTSA performed high mass impactor tests on the EUROSID-1, and EUROSID-1 with TNO Research Upgrade Kit and a prototype ball bearing rib design module from ASTC (EUROSID-1b) [3]. Subsequent EU 96/EC/27 crash tests of the EUROSID-1b, in coordinated research with Transport Canada, revealed that the rib deflection flat top problem was still present.

In May 2000, NHTSA responded to a petition for rulemaking by US industry and insurance groups, in effect to replace FMVSS 214 with the EU standard using an upgraded version of the EUROSID-1 dummy when it becomes available [4]. The agency granted the portion of the petition which requested that NHTSA consider replacing the side impact test dummy currently specified in the U.S. standard with an improved version of the dummy specified in the European regulation. All other aspects of the petition were denied.

The ES-2, the prototype upgrade of EUROSID-1, the side impact dummy of the European Union Side Impact Directive 96/EC/27, was developed by TNO Automotive to address mainly the following concerns and dummy response issues raised by users of the dummy worldwide [5,6]:

- "Flat tops" in the rib deflection responses, attributed mainly to binding in the rib modules and interference of the torso back plate
- Projecting back plate grabbing into the seat back
- Upper femur contact with the pubic load cell hardware
- Binding in the shoulder assembly resulting in limited shoulder rotation
- Spikes in the pubic symphysis load measurements associated with knee-to-knee contact

The main hardware upgrades introduced in the ES-2 dummy are [5,6]:

- An improved rib guide system in the thorax
- A curved and narrower back plate
- New attachment in the pelvis to increase the range of upper leg abduction and inclusion of rubber buffers
- A high mass flesh system in the legs
- Beveled edges in the shoulder assembly

The ES-2 offers the following instrumentation capabilities (Figure 1):

- Head accelerometer (tri-axial)
- Upper and lower neck load cell (6 axis)
- Clavicle load cell (tri-axial)
- Upper and Lower Spine accelerometer (tri-axial)
- Thorax rib deflection and accelerometer (uniaxial for each of the three ribs)
- Torso back plate load cell (4 axis)
- T12 load cell (4 axis)
- Abdomen load transducer (uniaxial: front, mid, and rear)
- Spine-Pelvis transfer load cell
- Pubic symphysis load transducer (uniaxial)
- Pelvis accelerometer (tri-axial)

- Left and right Femur load cell (6 axis)

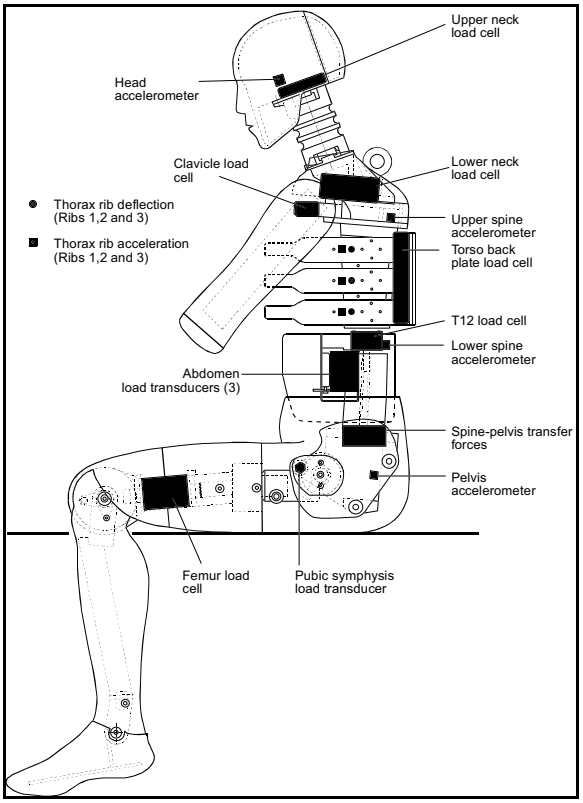

Figure 1. **ES-2 Instrumentation [8].**

The National Highway Traffic Safety Administration (NHTSA) is evaluating the ES-2 dummy to assess its performance in the FMVSS 214 test configuration. While differences in fleet compositions and crash involvement worldwide may preclude totally harmonized test conditions and movable barriers, the use of a single dummy in side impact standards worldwide would alleviate the current burdens of employing multiple test dummies in vehicle development and certification.

To understand the injuries which exist in the real world, this paper first presents results from NASS/CDS research into the side impact problem. Next, three types of impact experiments are presented - high mass impactor tests with the ES-2, full scale tests with the ES-2, and biofidelity sled tests with the SID and ES-2. Finally, an analysis of the repeatability of the ES-2 in the high mass impactor, vehicle, and sled tests is presented.

UNITED STATES SIDE CRASH ENVIRONMENT

In assessing the suitability of a dummy in a side impact test configuration, it is necessary to consider its injury assessment capabilities relative to human body regions at risk in the real world crash environment.

Methods

NASS/CDS years 1988-1999 were analyzed for light vehicles (GVWR under 10,000 lbs) a) with side damage b) that were not involved in a rollover event, and with c) minor secondary damage to the front, rear, or undercarriage of the vehicle.

FMVSS 214 mainly addresses thoracic and pelvic injuries and mandated a minimum of 10%, 25%, 40%, and full compliance of vehicle model years 1994, 1995, 1996, and 1997, respectively, of vehicles sold in the US. Thus, the injury distributions were then categorized based on annual averages of the crash data for vehicles of all model years up to 1994 from NASS/CDS years 1988-1995, and for vehicle model years 1995-1999, from NASS/CDS years 1996-1999.

Table 1.

NASS/CDS 88-99, all vehicle model years			
	All Crashes	Side Crashes (No Rollover)	Side Crashes (Subsequent Rollover)
vehicles	3,106,571	779,955	24,801
(%)		25.1%	0.8%
occupants, MAIS 3-6	115,793	30,719	3,215
(%)		26.5%	2.8%
injuries 3+	222,189	66,671	7,327
(%)		30%	3.3%

Table 2.

NASS/CDS 96-99, vehicle model years 95-99			
	All Crashes	Side Crashes (No Rollover)	Side Crashes (Subsequent Rollover)
vehicles	921,529	237,695	9,001
(%)		25.8%	1.0%
occupants, MAIS 3-6	27,019	6,446	1,141
(%)		23.9%	4.2%
injuries 3+	52,770	17,200	1,778
(%)		32.6%	3.4%

Results

Side crashes involve about 780,000 tow away vehicles per year in the United States (Table 1). These crashes involve

around 31,000 occupants with serious injuries. Occupants in side crashes tend to have more serious injuries than occupants of all crashes combined (Tables 1 and 2). When a modern crash fleet of vehicle model years 1995-1999 is considered, the seriously injured occupants in side crashes are 23.9% of the injured population, but they account for 32.6% of all the serious injuries (Table 2). In the modern side crash fleet where the crash partner is another light vehicle, the relative proportion of serious (AIS 3+) and severe (AIS 4+) thoracic injuries has decreased (Figures 2 and 3). The data shows a relative increase in serious injuries and severe injuries for the head and abdomen, and a relative increase in serious injuries in the pelvis.

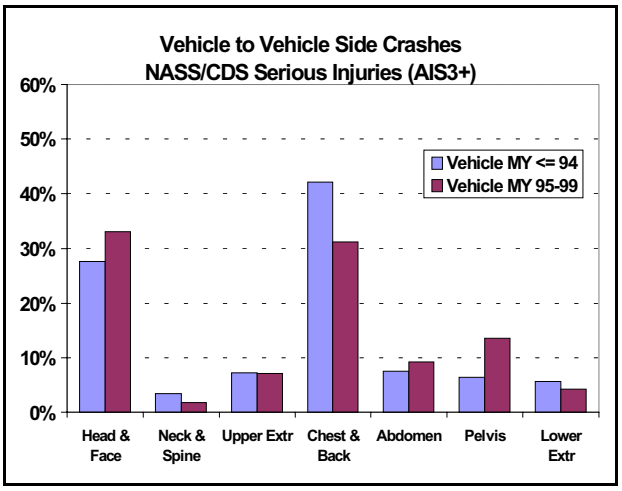

Figure 2. Distributions of serious (AIS 3+) injuries by body region for US side crashes based on NASS/CDS years 1988-1995 and 1996-1999.

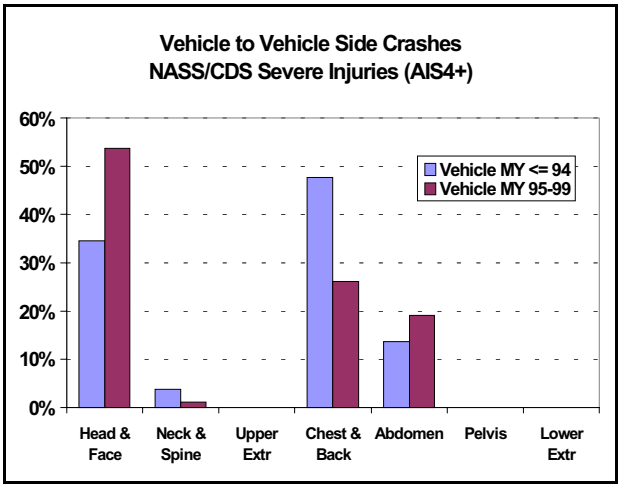

Figure 3. Distributions of severe (AIS 4+) injuries by body region for US side crashes based on NASS/CDS years 1988-1995 and 1996-1999.

Discussion

The apparent reduction in serious (AIS 3+) and severe (AIS 4+) thoracic injuries in vehicle to vehicle crashes between the MY94 and earlier vehicles and the MY 95-99 vehicles, may be attributed, in part, to the implementation of the US side impact standard, FMVSS 214. FMVSS 214 mainly addresses thoracic and pelvic injuries. Abdominal injuries also represent a significant number of severe injuries and are increasing with time, despite the implementation of FMVSS 214.

FMVSS 214 does not address head trauma, which represents a significant number of real-world injuries. Head trauma is addressed by FMVSS 201, Occupant Protection in Interior Impact. However, the focus of this paper is to address the responses of the ES-2 dummy in the current FMVSS 214 test configuration and as such it does not deal with the head and neck responses of the dummy. The ES-2 head and neck responses will be addressed, if needed, in other studies. Notwithstanding the head injuries in the modern US side crash fleet, improved measurement capabilities and injury criteria for the thorax, abdomen, pelvis, and if available for the lower and upper extremities in the side dummy of current FMVSS 214 should provide additional benefits in mitigating injuries in side crashes in the US.

ES-2 HIGH MASS IMPACTOR TESTS

Test Setup

The ES-2 prototype was initially introduced in early 2000 with three proposed rib designs intended to reduce friction in the rib guide bearings system:

- Coated piston: Standard EUROSID-1 ribs with PTFE (Poly-Tetra-Fluoro-Ethylene) coating, a polymer known for its extreme low friction properties
- Ball bearing: Guide system with spherical bearings (Advanced Safety Technologies Corporation, ASTC)
- Needle Bearing: Guide system with linear needle bearings (TNO)

To assess which rib design best addressed the flat top anomaly, a series of tests were performed with the ES-2 dummy fitted with each of the three proposed ribs designs using a high mass impactor test previously designed by NHTSA and MGA Research Corporation [2,3]. The high mass impactor test, shown in Figure 4, is designed to simulate the loading conditions in full-scale vehicle tests. The impactor is a Part 581 Bumper Testing Pendulum ballasted to 907 kg with linear springs attached between

the pendulum and the test frame to increase the impact speed.

The impactor face, covered with thick plywood sheet, was designed to engage the abdomen, thorax and the arm of the dummy just below the arm/shoulder interface joint. The ES-2 dummy was seated on a flat steel pedestal with legs extended and arm at 40 degrees. The impact angle was set using the neck mount of the dummy and the impactor surface as references. Impact angles were -10 degrees (rearward oblique), +10 and +20 degrees (frontal oblique), and a pure lateral impact at zero degrees. The focus was on the frontal oblique angles since the flat tops in the rib deflection were manifested in those angles in previous testing with EUROSID-1. The impact speed was approximately 18.3 kph.

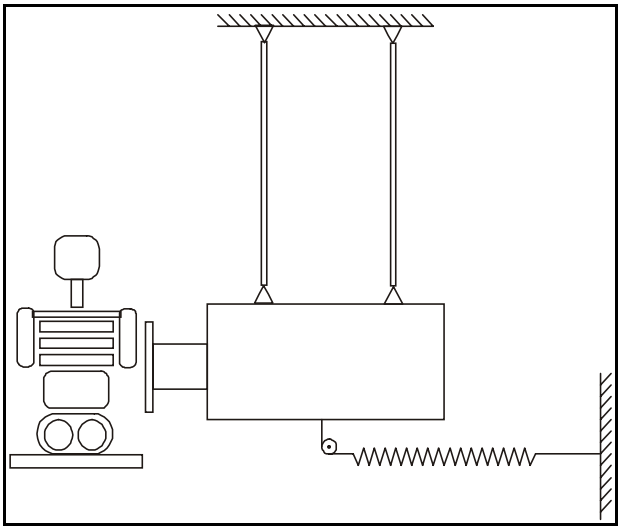

Figure 4. High Mass (907 kg) Pendulum Test Diagram

Test Results

Figures 5-8 present the rib deflections for the three designs at the four impact angles performed. The deflections, at each impact angle, are presented only for the middle or upper rib as examples since the other rib responses were similar with respect to the flat top.

For the coated piston rib design, the flat tops were still present in the rib deflections, more pronounced at the forward oblique angles of +10 and +20 degrees. For the ball bearing rib design, the flat top was substantially reduced and levels of deflection were increased. For the needle bearing design, the rib flat tops were not present at any of impact angles in the high mass impactor tests performed. The needle bearing design also resulted in higher deflections levels than the other two proposed rib designs.

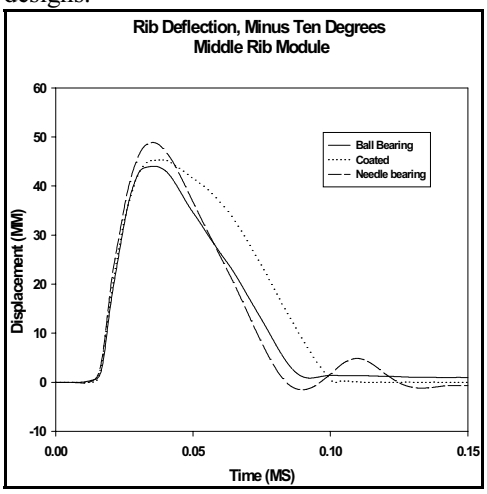

Figure 5.

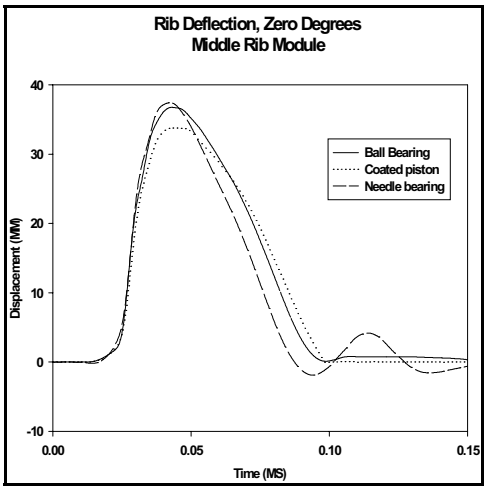

Figure 6.

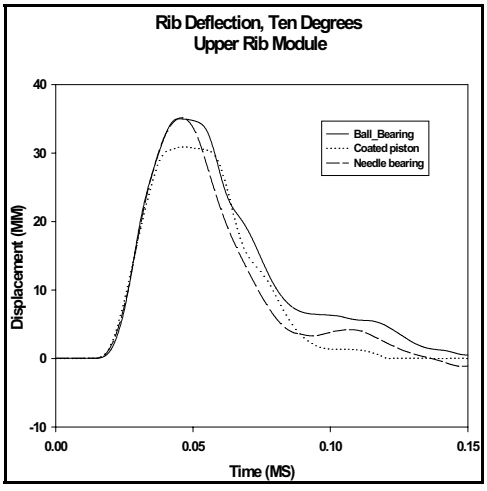

Figure 7.

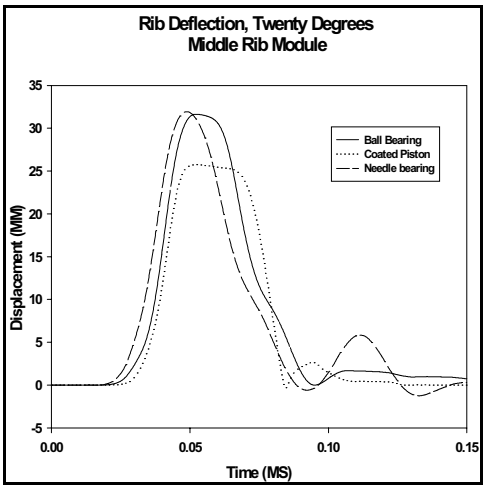

Figure 8.

ES-2 FULL SCALE CRASH TESTS

Table 3 presents the full scale test matrix which included both a front and rear seated ES-2 prototype dummies. The ES-2 with the needle bearing rib design was used in these tests as this rib design produced little or no rib deflection flat top behavior in the high mass impactor tests as described in the section above. The tests denoted with the asterisk ("*") were baseline tests performed with the EUROSID-1in 1997 in accordance with the EU 96/EC/27 side impact procedure, and were used to compare with the ES-2 responses in repeat test conditions. The US Side NCAP test condition was chosen to provide a higher severity loading environment for the ES-2. It is worth noting that both the Chevy Cavalier and the Pontiac Grand Am vehicles were chosen because of their marginal performance in the US Side NCAP with the US SID dummy. The full spectrum of ES-2 instrumentation was used in the full scale tests with the exception of the spine-pelvis transfer load cell (due to lack of availability).

Table 3. Full Scale Test Matrix

vehicle	dummy	test configuration	speed (km/h)
96 Taurus- 4dr*	Eurosid-1	EU Side	48.3
96 Taurus- 4dr	ES-2	EU Side	49.2
95 Metro- 3 dr*	Eurosid-1	EU Side	50.3
96 Metro- 3 dr	ES-2	EU Side	50.5
96 Taurus- 4dr	ES-2	FMVSS 214	53.3
96 Taurus- 4dr	ES-2	FMVSS 214	52.3
98 Chevy Cavalier- 4dr	ES-2	US Side NCAP	61.6
2000 Grand Am- 2dr	ES-2	US Side NCAP	62.1

Rib Responses (EU 96/EC/27)

Relative to the EUROSID-1 measures, there is an increase in the maximum rib deflections for the upper, middle, and lower ribs for the driver dummy in the EU Taurus and Metro tests with the ES-2, and a significant increase in the computed V*C values (APPENDIX A, Table A1).

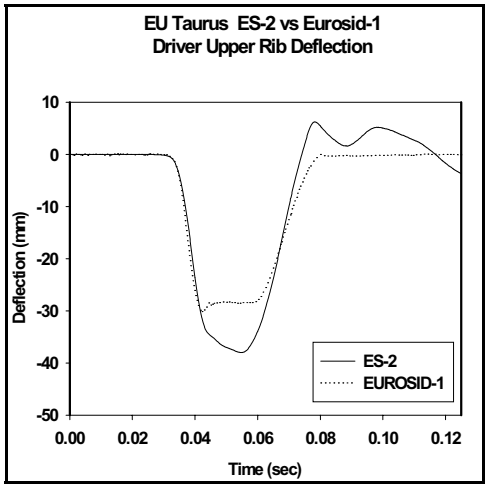

Figure 9.

In these two tests, the rib deflection flat tops have been reduced but are still present with the ES-2 dummy in the EU test configuration as exemplified by Figure 9 for the Taurus driver upper rib deflection and Figure 10 for the Metro driver middle rib deflection. There is no incidence of flat tops in the rib deflections for the rear passenger dummy for the ES-2 dummy in the EU tests performed (Figures 11 and 12).

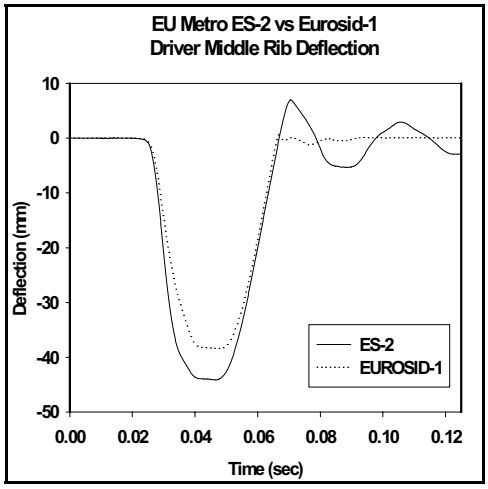

Figure 10.

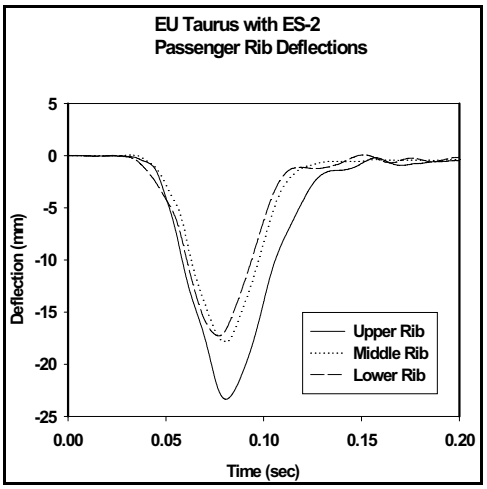

Figure 11.

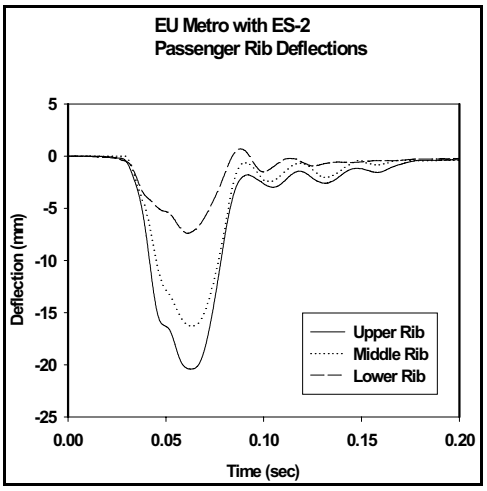

Figure 12.

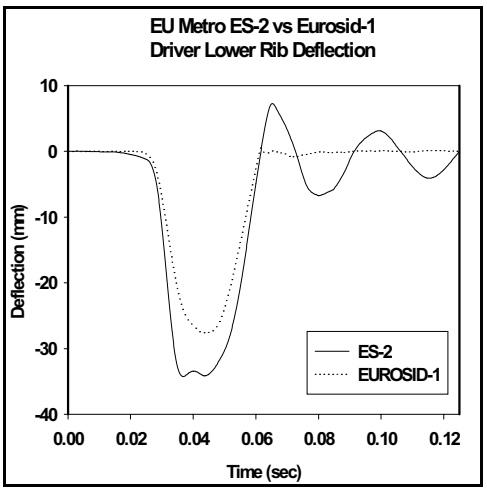

Figure 13.

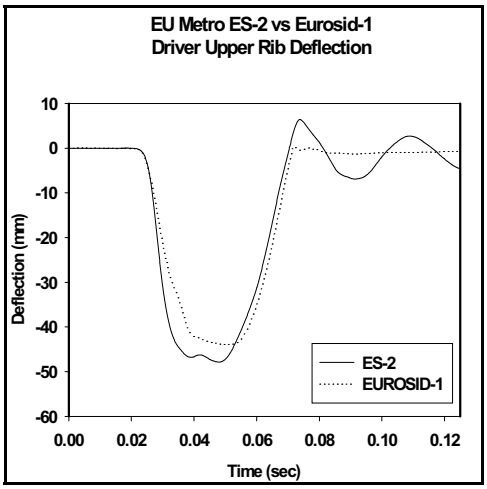

Figure 14.

The data in the Figures show post-event oscillations in the rib deflection responses for the ES-2, more predominantly for the driver dummy. There were also minor oscillations in the deflection near the peak for the Metro driver upper and lower ribs (Figures 13 and 14). This oscillatory behavior may be due to the reduced friction in the rib needle bearing guide design which leads to increased sensitivity to small variations in external loads. There is a good match in rib acceleration responses seen in this test series between the EUROSID-1 and ES-2, with the exception of peak values in certain cases (Figure 15 and 16).

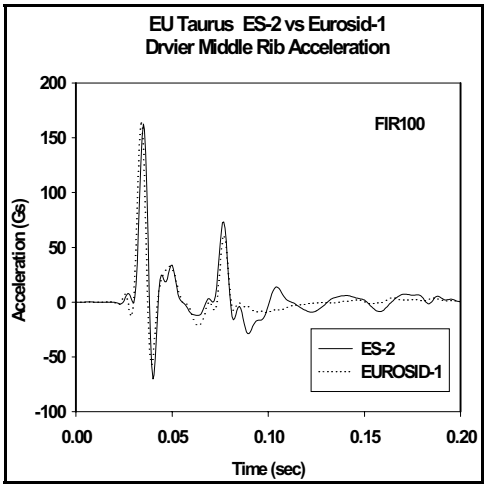

Figure 15

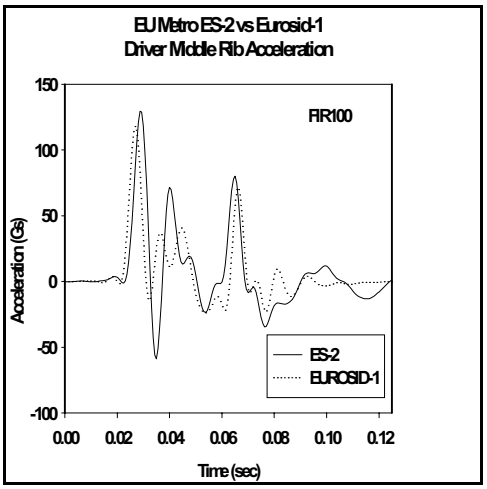

Figure 16.

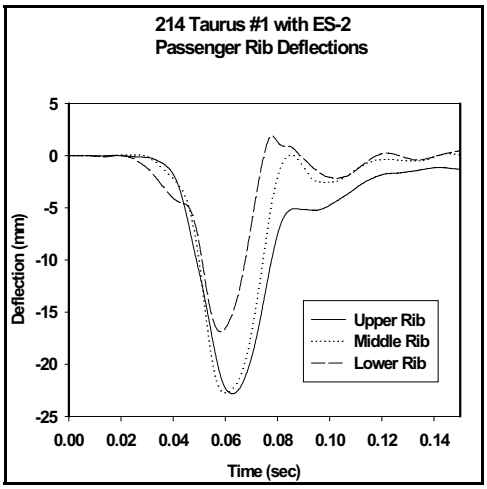

Figure 18.

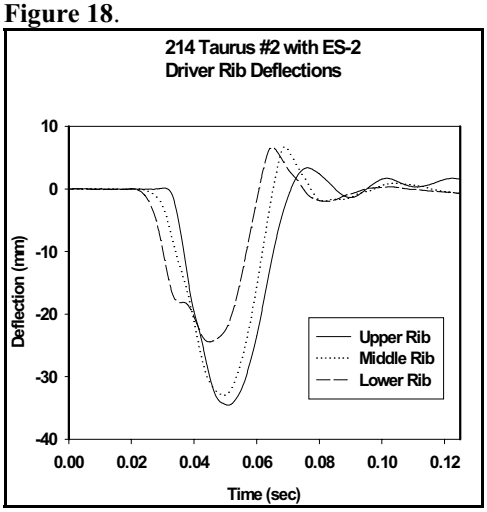

Figure 19.

Rib Responses (214/US Side NCAP)

Moderate values for both the peak rib deflections and V*C were measured in the FMVSS 214 tests for the driver dummy, and high values were measured in the US Side NCAP tests. Low values were measured for the rear passenger in both test conditions. The differences in rib values for the two repeat FMVSS 214 tests are discussed in a subsequent section in this paper.

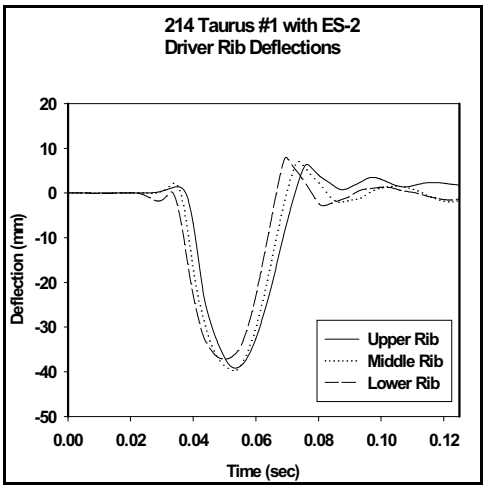

Figure 17.

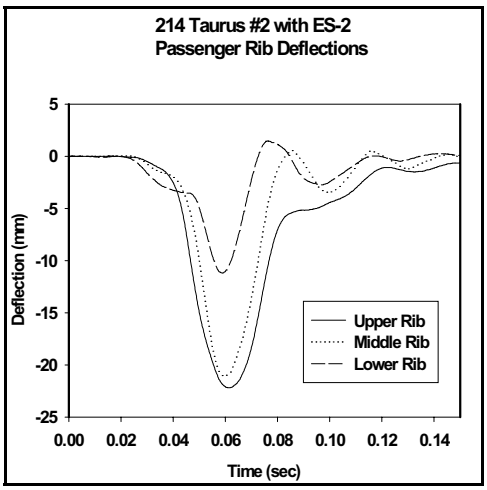

Figure 20.

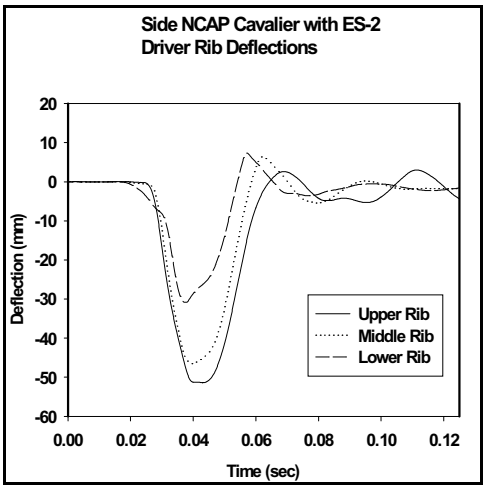

Figure 21.

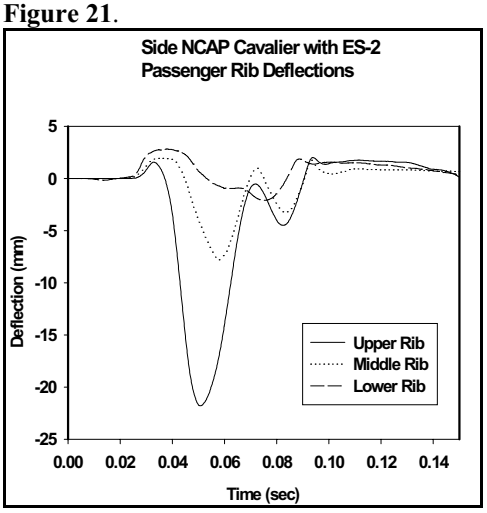

Figure 22.

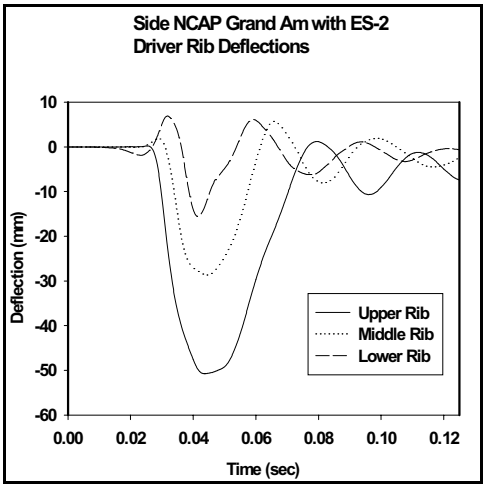

Figure 23.

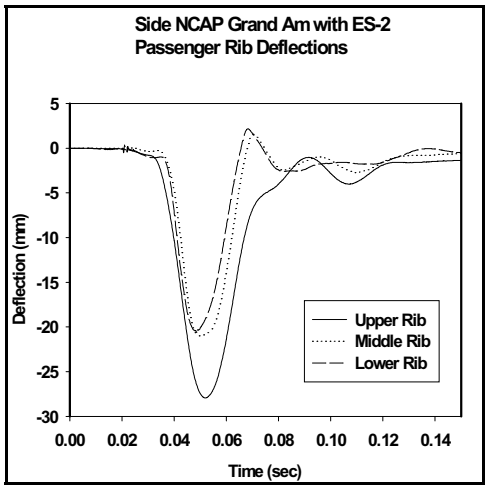

Figure 24.

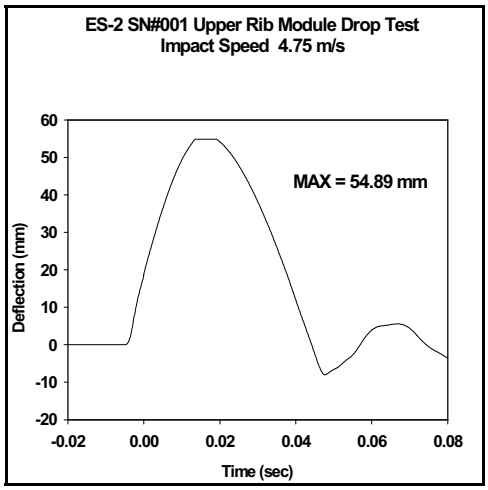

Figure 25.

Figures 17-24 present the rib deflections for the driver and passenger for the FMVSS 214 and Side NCAP tests with the ES-2. With exception of the Chevy Cavalier driver upper rib, there seems to be no incidence of flat top behavior in any of the ES-2 measured rib responses. The deflection response of the driver upper rib module was further investigated by performing additional rib certification drop tests [8] at higher impact velocities of 4.2,4.5, and 4.75 m/s. There was a slight amount of flat top in impact at 4.75 m/s at a deflection level of 55 mm (Figure 25). A repeat drop test at the high impact velocity indicated that the maximum effective dynamic range of the ribs is around 55 mm.

The ES-2 rib accelerations from the first Taurus FMVSS 214 test and the US Side NCAP Chevy Cavalier test are presented in Figures 26 and 27. These are typical of the ES-2 rib accelerations seen in these tests.

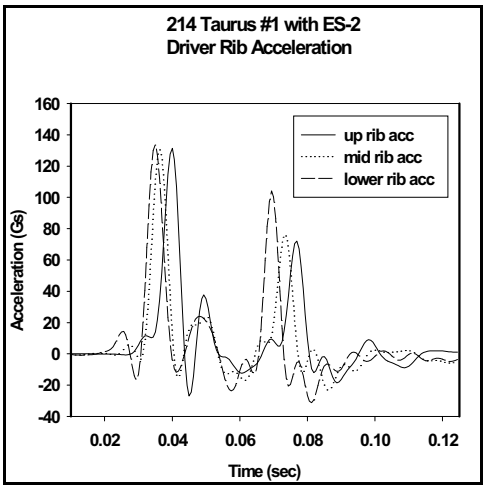

Figure 26.

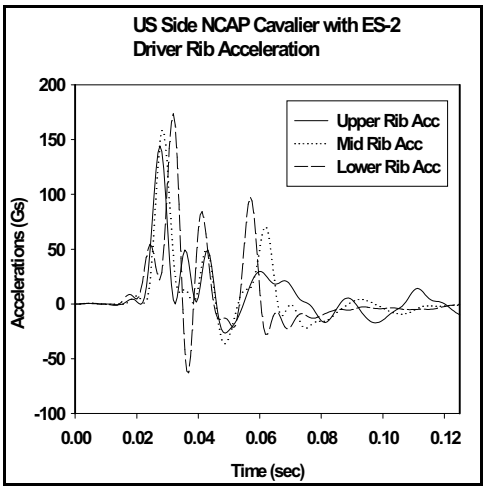

Figure 27.

Summary of Rib Responses - Further testing is needed to investigate whether flat tops and the 55 mm dynamic range limit of the ES-2 rib deflection measurement become an issue in the US Side NCAP test conditions. This will need to be assessed in relation to future chest deflection criterion developed for the ES-2 dummy.

Pelvic Responses (EU 96/EC/27)

There is considerable reduction in the pubic symphysis forces (PSF) for the ES-2 dummy relative to the EUROSID-1 in the EU test condition (Table A2 and Figures 28-31). The ES-2 pubic load responses are synchronized in time with those of the EUROSID-1 and have similar signal shapes, but are simply at reduced levels for these two sets of repeat tests. Similar observations apply to the pelvic acceleration, shown for the EU Taurus as an example, in Figures 32 and 33, although there is less increase in peak accelerations for the ES-2 relative to the EUROSID-1.

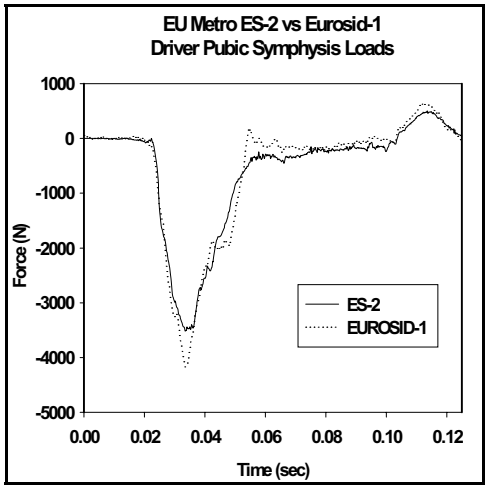

Figure 28.

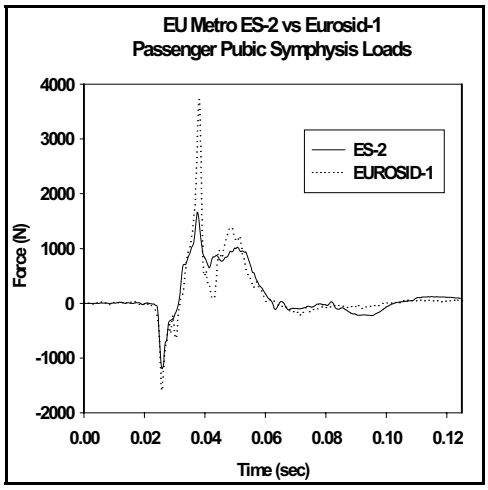

Figure 29.

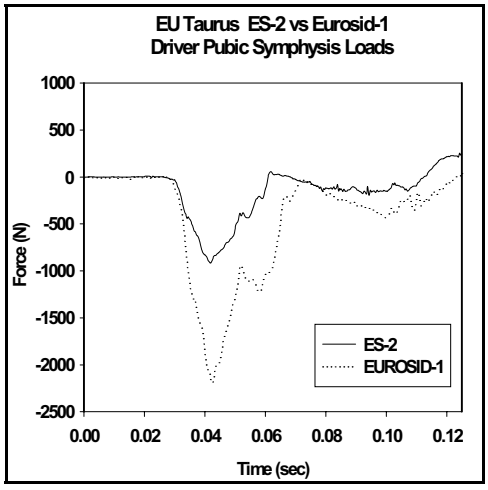

Figure 30.

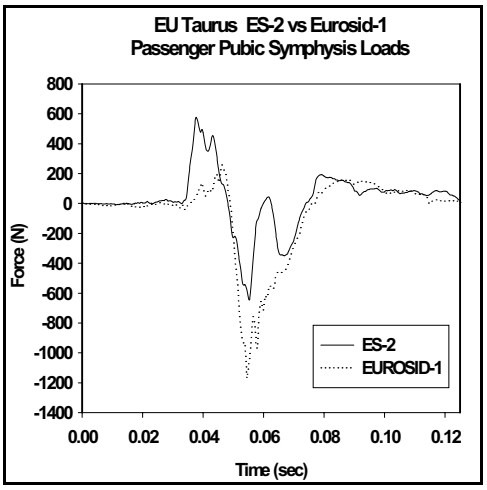

Figure 31.

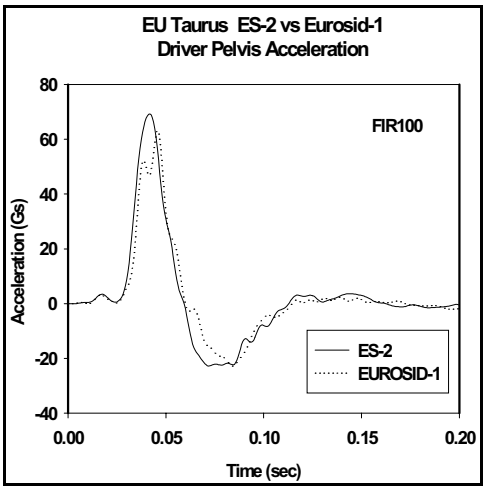

Figure 32.

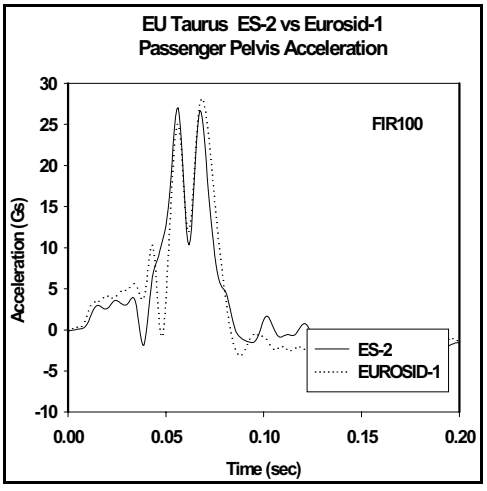

Figure 33.

To investigate the occurrence of knee-to-knee contact and the resulting effect on pubic loads, the femur loads were examined for spikes in the x, y, and z components around the time of increasing but opposite loads observed in the left and right lateral femur load components. It is presumed that the knee-to-knee contact can lead to an oscillatory/ringing effect that travels up the femurs and leads into the PSF. Presuming that such spikes are an indication of knee-to-knee contact, the pubic symphysis loads were then examined for increased levels around the time of knee-to-knee contact. For the two EU tests performed, the data shows some knee-to-knee contact for ES-2 dummy but suggests little or no effect on the corresponding ES-2 peak pubic loads. For example, there is a slight increase in the PSF peak at the time of occurrence of the minor data spikes in the femur loads for the ES-2 driver in the EU Taurus test (Figure 34).

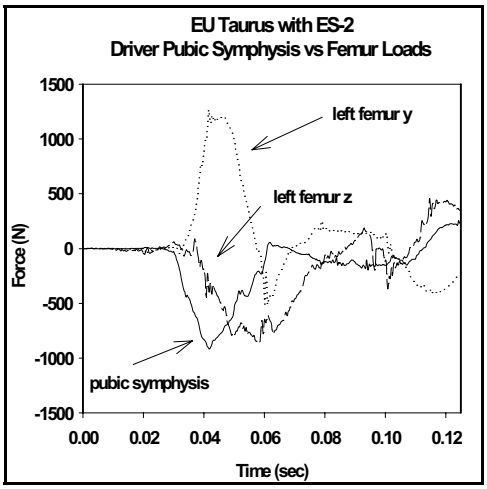

Figure 34.

Pelvic Responses (214/US Side NCAP)

The PSF levels were low for both the driver and rear passenger ES-2 in the FMVSS 214 tests. PSF levels were also low for the driver in the US Side NCAP tests while high, in the range of 5-6 kN, for the rear passenger ES-2. Figures 35 and 36 present a good match of the PSF responses in the two FMVSS 214 Taurus tests for both the driver and passenger. A very good match was seen for the pelvis accelerations in the FMVSS 214 repeat tests.

There is a minor increase on the PSF peak levels for both the driver and passenger ES-2, for FMVSS 214 Taurus test #2, at the time of knee-to-knee contact as observed from the over plots of the femur loads (Figures 37 and 38). Similar results were seen for FMVSS 214 Taurus test #1.

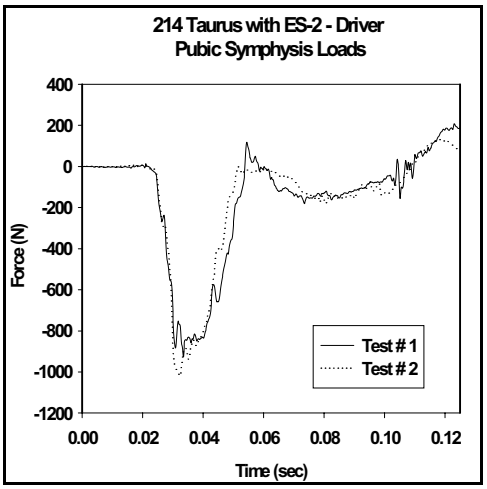

Figure 35.

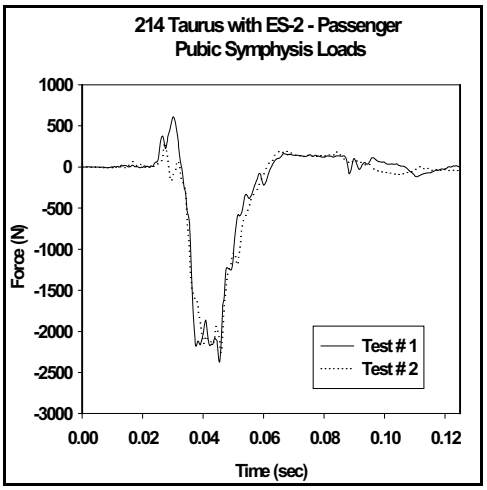

Figure 36.

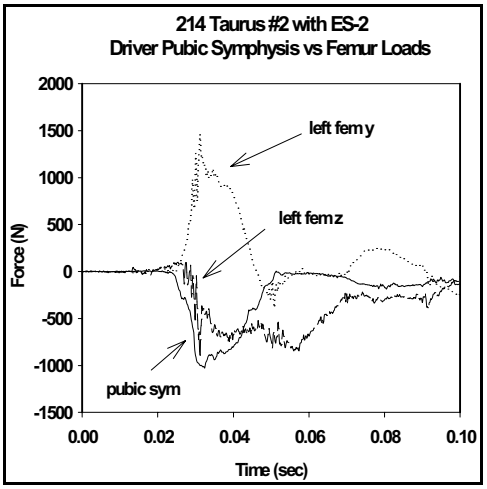

Figure 37.

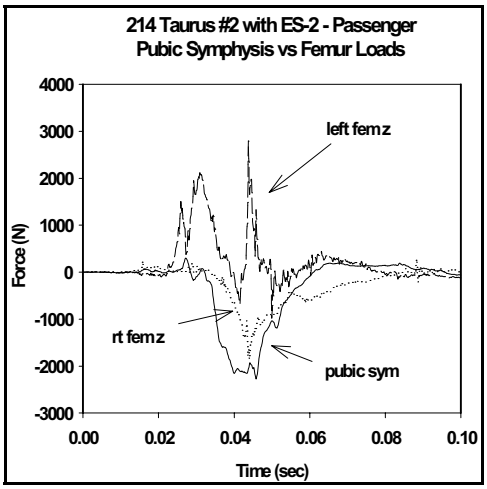

Figure 38.

There was no noticeable effect on the PSF peak values from the spiky responses of the left femur loads at knee-to-knee contact for the US Side NCAP Chevy Cavalier driver (Figure 39), however, there was a noticeable effect in the passenger PSF response (Figure 40). For the Cavalier passenger, this did not occur at the same time of the peak PSF response and thus did not contribute to the peak value. There was no effect on the PSF responses for the driver ES-2 in the US Side NCAP Grand Am tests, while there seems to be a small effect on the main peak PSF value for the rear passenger ES-2 (Figures 41 and 42).

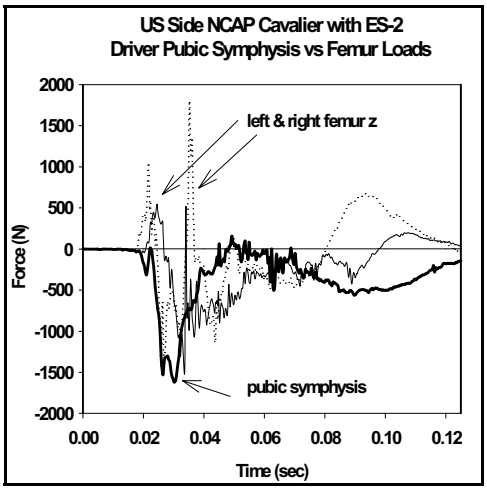

Figure 39.

The phenomenon of knee-to knee contact was further investigated in the sled tests performed with the ES-2 dummy for biofidelity assessment (Refer to section on biofidelity later in the paper). In two of the thirteen sled tests (the rigid low speed flat wall and the rigid abdominal

offset), the knee-to-knee contact seemed to cause a large irregular spike in the PSF. Both of the spikes seem to coincide with the left femur z force output. There was no effect on the peak PSF values in any of the thirteen sled tests performed, however there seems to be other minor segments in the PSF signals where knee-to-knee contact leads to alterations in the overall pubic load.

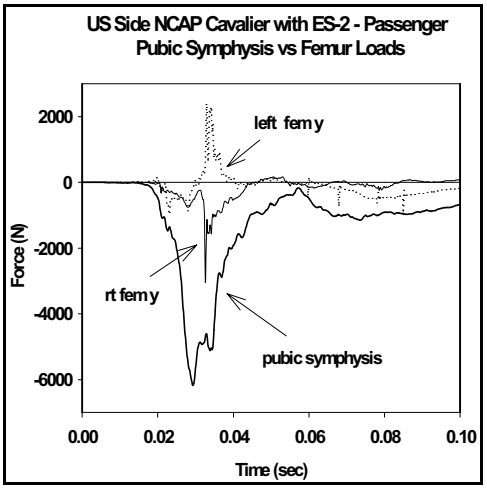

Figure 40.

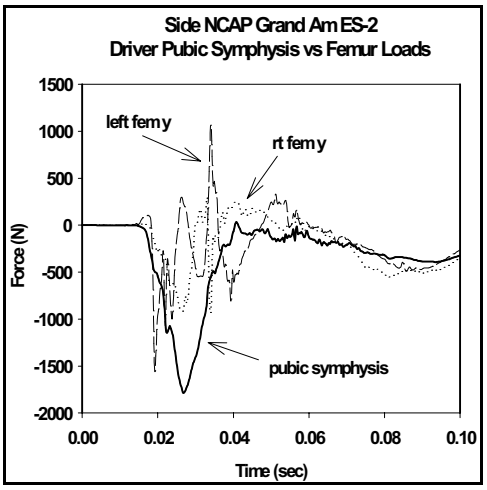

Figure 41.

Overall, the data in the full scale and sled tests performed suggests that knee-to-knee contact in the ES-2 dummy has little or no effect on increasing the pubic symphysis loads. However, the knee-to-knee contact may cause minor effects to the PSF signal such as abnormal spiking. Additional full scale tests would further investigate this phenomenon.

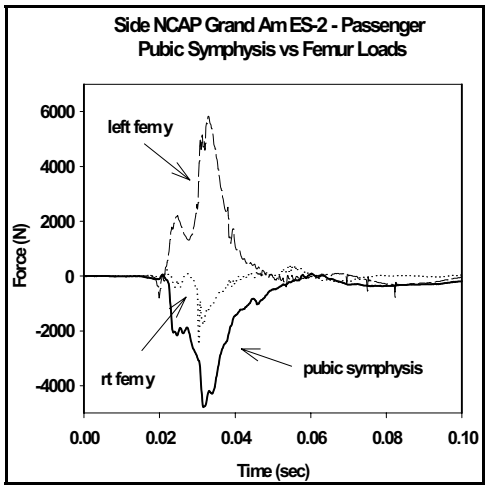

Figure 42.

Abdominal Loads

The abdominal loads increased considerably for both the driver and passenger in the EU Taurus test with ES-2 dummy relative to the EUROSID-1 while they decreased for the Metro driver and stayed relatively the same for the Metro rear passenger (Figures 43-46). The abdominal loads were relatively high for the driver and passenger ES-2 dummies on both the FMVSS 214 and US Side NCAP tests .

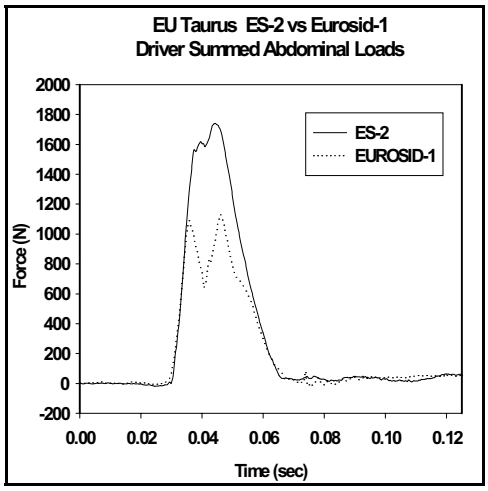

Figure 43.

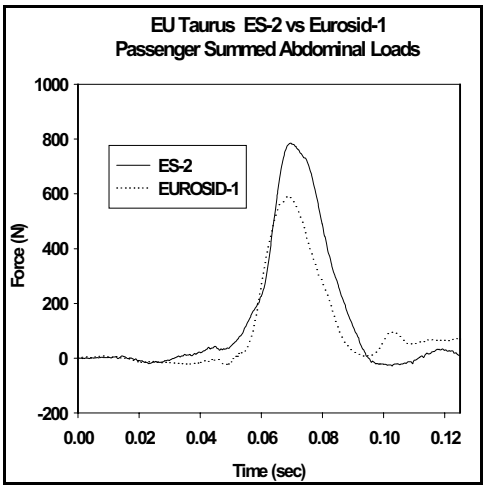

Figure 44.

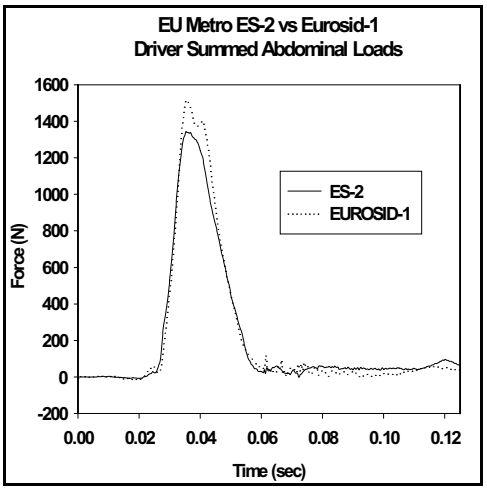

Figure 45.

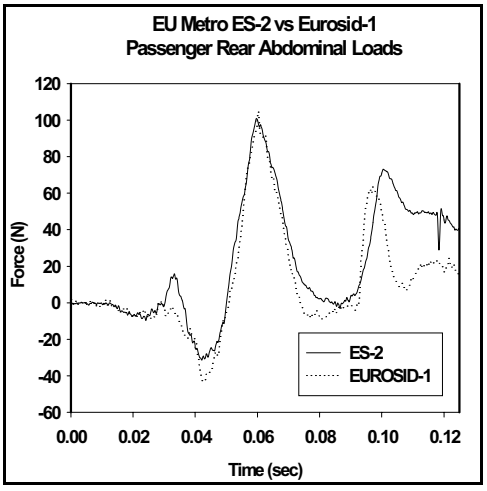

Figure 46.

BACK PLATE LOADS

The ES-2 has a load cell which measures the x and y forces, and y and z moments between the back plate of the ES-2 and the spine. The back plate typically carries the loads delivered by the seat back to the dummy. Considerable back plate loads have been observed in the full scale test performed for both the driver and passenger ES-2 dummies (Tables 4 and 5).

Table 4. Driver Back Plate Peak Loads & Moments

vehicle/test	F_x	F_y	M_y	M_z
all CFC 600	**(N)**	**(N)**	**(N-m)**	**(N-m)**
EU Taurus/EUROSID-1				
EU Taurus/ES-2	179	**-316**	-8	**11**
214 Taurus #1/ES-2	433	**-511**	23	**24**
214 Taurus #2/ES-2	399	734	18	13
EU Metro/EUROSID-1				
EU Metro/ES-2	241	-450	-10	15
NCAP Cavalier/ES-2	1168	889	30	43
NCAP Grand Am/ES-2	265	-658	8	8

A positive longitudinal load, $\mathbf{F_x}$, indicates that the backplate is being pushed forward. A positive lateral load, $\mathbf{F_y}$, indicates that the backplate is being pushed to the right. A positive $\mathbf{M_y}$ indicates that the bottom half of the backplate is being pushed and the top half is being pulled. A positive $\mathbf{M_z}$ indicates that the left half of the backplate is being pushed and the right half is being pulled.

Table 5. Passenger Back Plate Peak Loads & Moments

vehicle/test	F_x	F_y	M_x	M_y
all CFC 600	(N)	(N)	(N-m)	(N-m)
EU Taurus/EUROSID-1				
EU Taurus/ES-2	317	197	0	13
214 Taurus #1/ES-2	1413	-503	**-99**	**-55**
214 Taurus #2/ES-2	1687	-843	**-120**	**-82**
EU Metro/EUROSID-1				
EU Metro/ES-2	347	2328	**181**	**158**
NCAP Cavalier/ES-2	1510	-1035	**-55**	**-22**
NCAP Grand Am/ES-2	268	-1033	-8	7

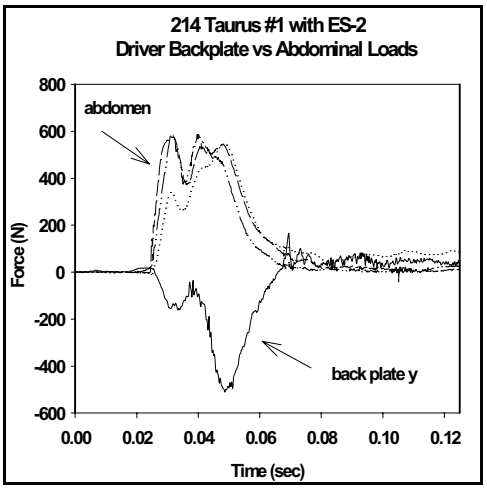

Figure 47

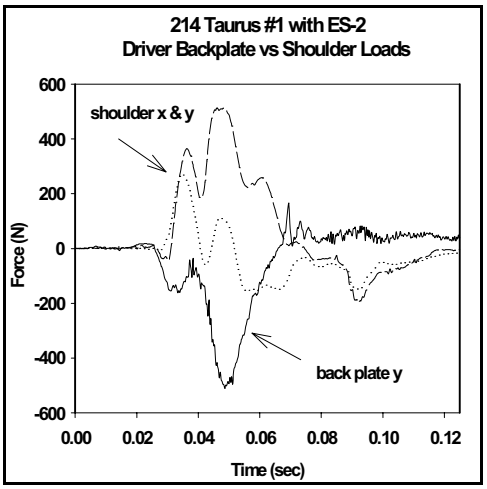

Figure 48.

Figures 47-51 present some of the back plate lateral loads in comparison with other dummy loads. It is noted that the EU Metro passenger back plate lateral loads were very large compered to the other dummy loads.

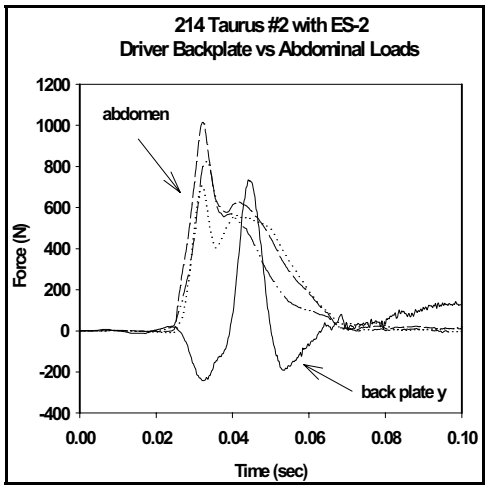

Figure 49.

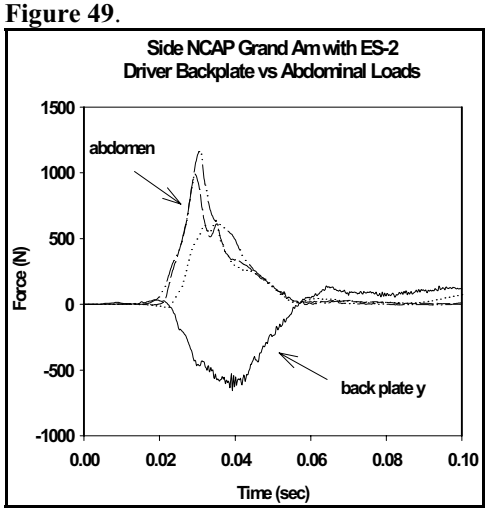

Figure 50.

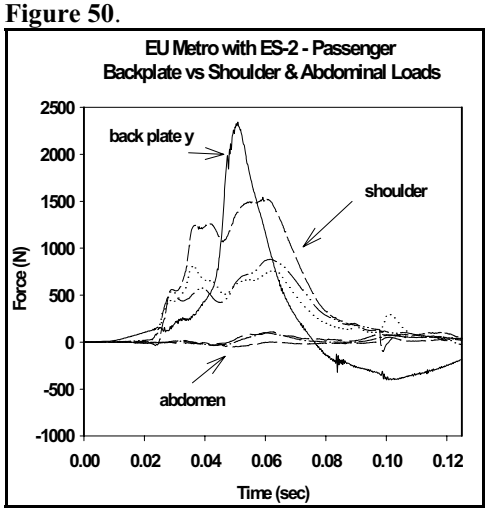

Figure 51.

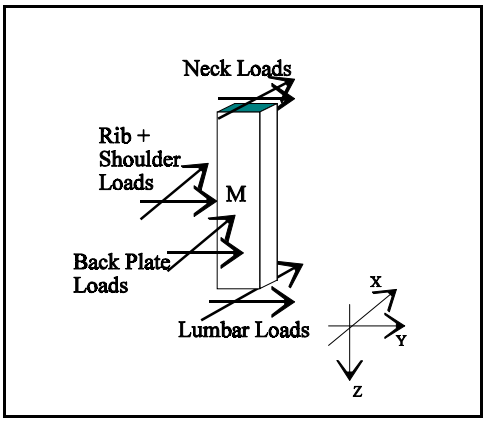

Figure 52- Free body diagram of ES-2 Spine, showing 4 external loads - those from neck above, the lumbar spine from below, the back plate from the rear, and loads from the ribs and shoulder from the left. Coordinate system is SAE J211 - x forward, y right, z down.

Analysis of Back Plate Loads

To investigate back plate interaction with the seat back, an analysis was performed to compare the back plate loads to other forces acting on the ES-2 during the crash test.

Methods - Constructing a simple free-body diagram of the ES-2 Spine (Figure 52) yields four external loads, those from neck above, the lumbar spine from below, the back plate from the rear, and loads from the rib and shoulders from left. Integrating Newton's second law of motion,

$$\sum \int_{t_1}^{t_2} F dt = m \int_{t_1}^{t_2} a dt$$

and then applying to the ES-2 spine free-body diagram, yields:

$$m\Delta V_{t_1\ spine}^{t_2} = \int_{t_1}^{t_2} F_{Lumbar}\,dt + \int_{t_1}^{t_2} F_{Backplate}\,dt + \int_{t_1}^{t_2} F_{Rib+Shoulder}\,dt + \int_{t_1}^{t_2} F_{Neck}\,dt \quad \text{Eq 1}$$

which is linear momentum-impulse balance between the spine and the external loads applied to it. In all of the ES-2 crash tests performed, load cells data is available at the lumbar spine, back plate, and neck, as well as accelerometers at the upper and lower spine. Therefore, there is sufficient information to solve Equation 1 for the unknown load $F_{rib+shoulder}$. A similar *angular* momentum-impulse balance could have been performed, however there is not sufficient instrumentation to determine the rotational acceleration of the spine.

Equation 1 was applied to the six ES-2 crash tests performed, and the impulse applied by rib and shoulder was calculated for each test. The mass of the ES-2 spine was assumed to be 20 kg, which includes the spine itself, and the rigid rib components on the non-struck side of the thorax. Integration limits t_1 and t_2 were determined from observation of beginning and end, respectively, of rib deflection and pelvis force signals.

Results- In the X direction, the driver and passenger back plate loads delivered positive impulses in all tests except one, while the ribs and shoulder delivered negative direction loads in all but two cases (Figure 53). In the Y direction, ribs and shoulder impulses were positive in all cases, while the back plate loads were mixed in direction (Figure 54). Y direction rib and shoulder impulses were always greater than any other impulse source. Y Rib and shoulder impulses were higher on average for the driver than for the passenger (Figures 54, 56). X direction rib and shoulder impulses were lower for the driver and mixed in direction, while for the passenger rib and shoulder impulses were much higher in magnitude and always negative (Figures 53, 55).

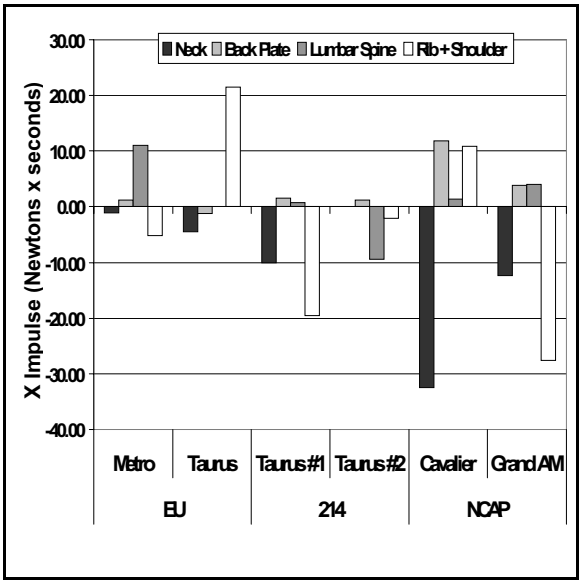

Figure 53. Driver X Direction Impulse of Neck, Back Plate, Lumbar Spine and Rib loads applied to ES-2 Thoracic Spine, from full-scale vehicle crash tests. Positive impulse vector points forward.

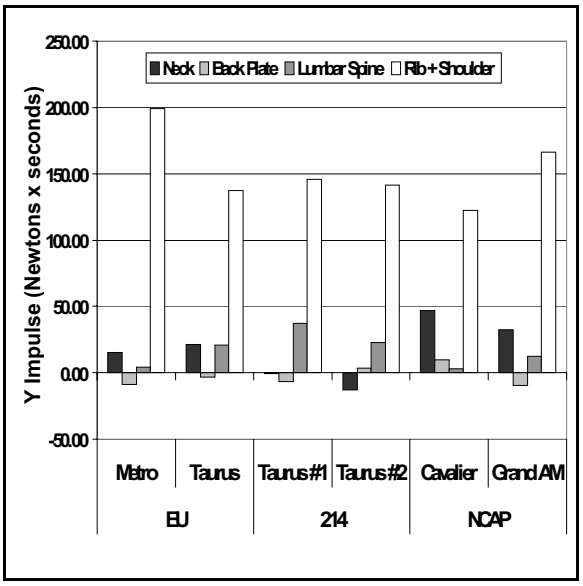

Figure 54. Driver Y Direction Impulse of Neck, Back Plate, Lumbar Spine and Rib loads applied to ES-2 Thoracic Spine, from full-scale vehicle crash tests.

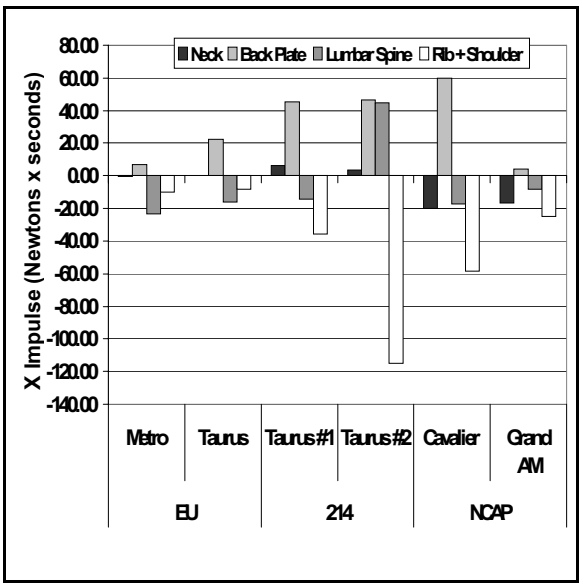

Figure 55. Passenger X Direction Impulse of Neck, Back Plate, Lumbar Spine and Rib loads applied to ES-2 Thoracic Spine, from full-scale vehicle crash tests. Positive impulse vector points forward.

Discussion of Back Plate Loads

Compared to the rib and shoulder load, the contribution of the lumbar, neck and backplate loads to the acceleration of the dummy is relatively minimal. Moreover, the back plate contributes no more to the overall acceleration of the dummy than do the neck or lumbar loads. This suggests that seat back grabbing on the back plate of the ES-2 contributes no more to the response of the dummy than does, say, the loads on the thorax structure by the head/neck complex. Compared to the driver, rear passenger x direction rib and shoulder loads are quite high and directed towards the rear. This is a result of the rearward door intrusion vector often observed in lateral crash tests. The high back plate impulses directed forward further confirm this, as they are an indication that the dummy is being pressed into the seat by the door. The driver X loads were quite low and mixed in direction, indicating a laterally intruding door vector in the driver position.

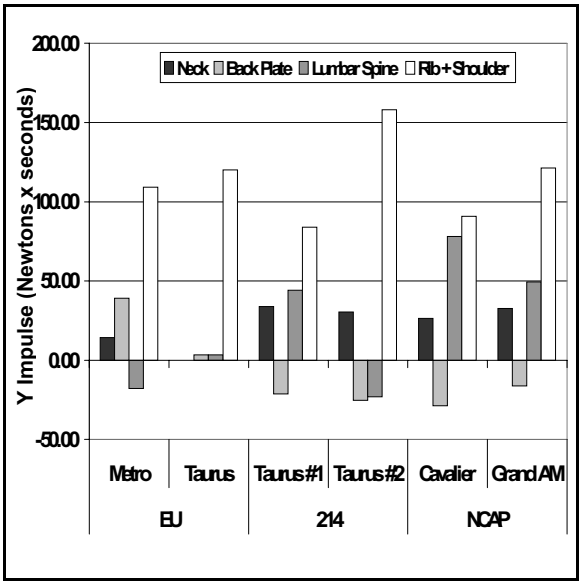

Figure 56 - Passenger Y Direction Impulse of Neck, Back Plate, Lumbar Spine and Rib loads applied to ES-2 Thoracic Spine, from full-scale vehicle crash tests. Positive impulse vector points forward.

Despite the above analysis, we have no information which evaluates the biofidelity of the back plate in its interaction with the seat. The significance and effect of back plate loading on peak dummy responses, including rib deflections has not been assessed. Further, the SID does not have the capability to measure back plate loads, so we have no way of comparing the SID seat back-to-dummy interaction with that of the ES-2. The above analysis merely relates the magnitude, duration and direction of loads exchanged between the seat back and the ES-2 with the other loads governing the kinematic response of the dummy.

BIOFIDELITY ASSESSMENT OF ES-2 RELATIVE TO THE SID

An important aspect of evaluating the ES-2 dummy in the FMVSS 214 test configuration is the assessment of its biofidelity, in particular relative to the SID.

Biofidelity Assessment Methods

To provide a basis for determining the biofidelity of these anthropomorphic crash dummies, a series of sled impact experiments were performed on post-mortem human subjects (PMHS) in crash conditions similar to a full scale vehicle impacts. Forty five sled side impact cadaver tests were conducted. The methodology used to analyze these data is presented in Appendix B. The following sled tests were conducted: rigid 8.9 m/s flat wall, padded 8.9 m/s flat wall , rigid 6.7 m/s flat wall , padded 6.7 m/s flat wall , rigid 6.7 m/s abdominal offset test (arm up), and padded 6.7 m/s pelvic offset tests. The dummies were tested in the same impact conditions as the PMHS. For the PMHS and dummy tests, kinetic and kinematic measurements were sampled in time on both the test subject and the test apparatus during the impact event. The measurements on the dummies were then compared with the averaged responses on the PMHS.

For each of the forces, accelerations and thoracic deflections, the techniques of Morgan [9] were modified slightly to quantify dummy biofidelity with respect to these corridors. First, time-zero was determined in each dummy impact test in the same manner as the analysis in Appendix B. That is, for the flat wall tests, time-zero occurred when the occupant made contact with the thoracic load plate. For the pelvis and abdomen offset tests, time-zero was determined as when the occupant strikes the pelvis and abdomen load plates, respectively.

Table 6- Ratio of DCV to CCV for the ES-2 and the SID by test condition.

		WALL->	Flat Wall								Abd. Offset		Pelvis Offset			
		SPEED->	8.9 m/s				6.7 m/s				6.7 m/s		6.7 m/s			
		PAD->	Rigid Wall		Padded Wall		Rigid Wall		Padded Wall		Rigid Wall		Rigid Wall		MEAN***	
		DUMMY	ES-2	SID	ES-2	SID	ES-2	SID	ES-2	SID	ES-2	SID*	ES-2	SID	ES-2	SID
MEASUREMENT	FORCE	THRX	14.6	11.2	8.50	8.42	8.82	7.69	6.99	2.04	0.31		5.56	0.77	8.89	6.02
		ABDM	4.17	2.41	7.18	7.19	0.49	0.67	2.52	3.00	19.2		0.23	0.45	2.92	2.74
		PELV	cf	5.54	cf	9.36	2.84	1.31	2.71	2.17	3.23		0.42	1.74	1.99	1.74
		LEGG	8.77	2.30	6.17	3.81	12.4	5.08	6.52	3.32	6.06		2.86	1.72	7.33	3.24
	DEFL**	UPPER	0.98		1.75		4.18		0.40		cf		5.62			
		LOWER	3.05		0.19		4.40		0.47		2.85					
	ACCELERATION	RBLU	1.90	1.71	1.15	1.02	0.44	0.67	0.73	0.56	3.71		1.93	1.25	1.23	1.04
		RBLL	2.41	0.55	0.73	1.49	0.79	1.39	0.43	0.55	0.79		1.67	0.56	1.20	0.91
		SPNU	1.77	1.91	1.90	2.51	1.57	1.59	1.38	1.23	3.31		1.36	2.02	1.60	1.85
		SPNL	2.27	1.12	1.59	1.04	3.11	2.40	0.90	0.52	6.57		cf	cf	1.97	1.27
		PVSA	3.50	2.33	3.20	1.98	2.81	1.55	3.95	1.27	0.88		2.12	2.57	3.11	1.94
		MEAN***	4.92	2.94	3.80	3.43	3.69	2.48	2.90	1.63			2.02	1.38		

Measurement Key: THRX = Thorax, ABDM = Abdomen, PELV = Pelvis and LEGG = Leg Load Wall Force, respectively. UPPER = ES-2 Upper Rib Deflection, LOWER = ES-2 Lower Rib Deflection. RBLU = Left Upper Rib, RBLL = Left Lower Rib, SPNU = Upper Spine, SPNL = Lower Spine, and PVSA = Pelvis Acceleration, respectively. MEAN is the mean dummy response for a particular row or column.

NOTES: cf = data channel failure.
"*" = No SID test run.
"**" = SID was not instrumented with chest pot for these tests.
"***" = MEAN is only calculated for cases where both an ES-2 and SID measurements are available.

As previously defined by Morgan, the cadaver cumulative variance (CCV) and the dummy cumulative variance (DCV) were calculated. The CCV is a measure of the standard deviation of a particular group of cadaver transducer signals, over time. The DCV is a measure of how much a dummy transducer signal varies from the mean cadaveric response over time. The ratio DCV/CCV is the number of cadaver standard deviations a dummy signal varies from the cadaver mean. In some cases, more than one test was run for a given dummy in a particular test condition, and thus the DCV/CCV ratio was averaged where repeat dummy tests were available.

The specific measurements to be considered in biofidelity assessment is a matter of importance. In the case of a side crash similar to the FMVSS 214 test configuration, an intruding door impacts the lateral aspects of the shoulder, arm, thorax, abdomen, pelvis, and legs of a seated occupant. Both the response of the occupant and the response of the vehicle interior should be considered in assessing biofidelity. For the dummy and human occupants, the forces applied to the vehicle interior by the occupant should be compared, both in magnitude and time, as well as contact area and location. In addition, those measurements necessary for calculation of injury criteria should also be evaluated.

Biofidelity Assessment Results

DCV/CCV ratios are presented in Table 6. Row and column means were calculated for all test conditions where both a SID and ES-2 signals were available. The internal loads on the ES-2, such as pubic symphysis and abdominal loads, were not included in the biofidelity analysis as these quantities were not measured on the cadaver. There is no data for the SID in the abdominal offset condition as this test was not performed. There is no ES-2 pelvic wall force data due to instrumentation failure in the rigid and padded wall high speed tests. Also, there is no SID chest deflection data since the SID was not instrumented to measure chest deflections.

For many of the signals analyzed, the shape and magnitude of the dummy responses was quite similar to the cadaver corridor, as exemplified in Figures 57-60. However, because of phase differences between the cadaver corridors and the dummy signals, the dummy signals varied from the cadaver mean by several standard deviations , and thus DCV/CCV ratios were relatively large (Table 6).

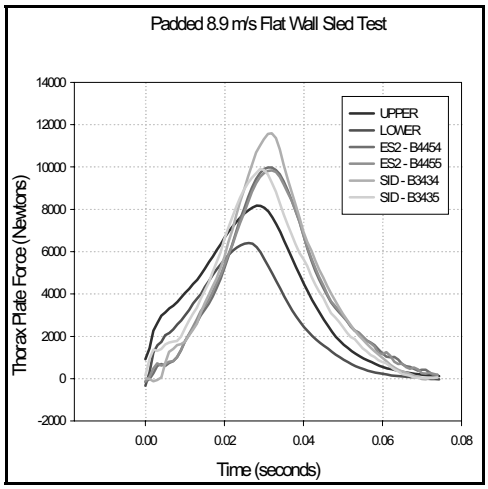

Figure 57.

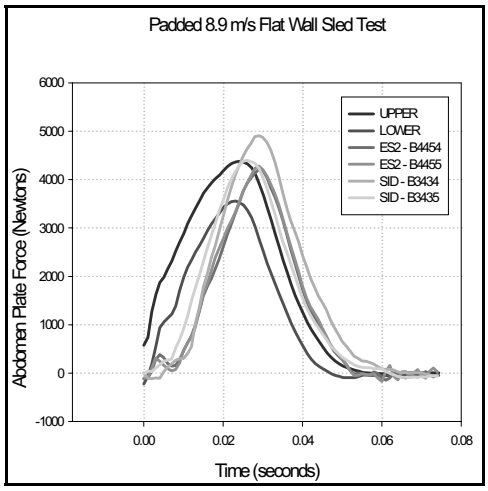

Figure 58.

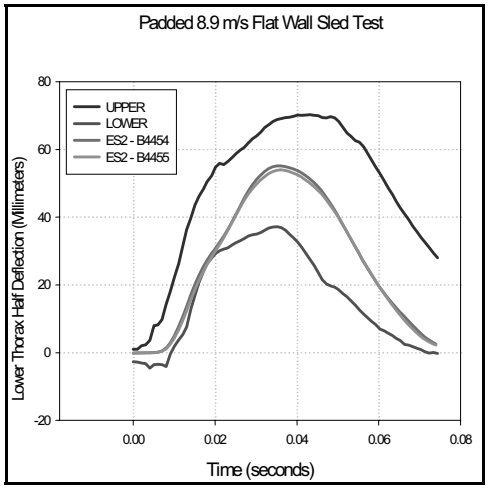

Figure 59.

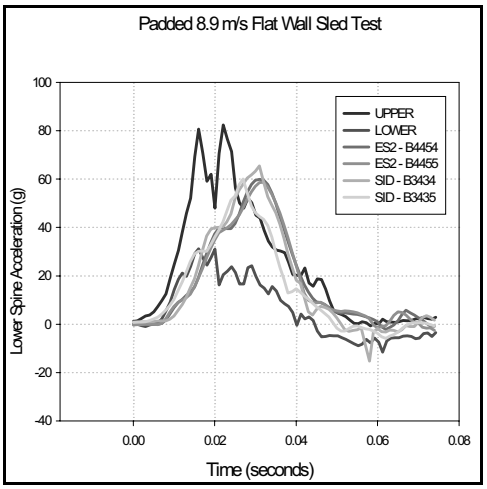

Figure 60.

Biofidelity Assessment Discussion

Recent work by Kuppa et al [7] demonstrated the importance of thoracic deflection in injury prediction, however the SID was not instrumented to measure deflection in this test series. Real world crash analysis data presented earlier in this study showed a substantial number of serious abdominal injuries in vehicle side impacts. The SID and the ES-2 have nearly similar force biofidelity in the abdomen (Table 6, ABDM Row), however the ES-2 offers abdominal measurement capability, while the SID does not. The SID and the ES-2 also have similar force biofidelity in the pelvis region, however the ES-2 offers measurement of pubic symphysis loads as well as pelvis acceleration, while the SID offers only pelvis acceleration.

To provide a more complete assessment of biofidelity, future tests of the ES-2 and SID will be conducted. Further, biofidelity should not be the only factor considered when selecting the best device to assess injury. Measurement capability, repeatability, reproducibility, durability, dummy handling and other factors must be considered before selecting a crash test dummy.

ES-2 REPEATABILITY

Rib Deflections in High Mass Impactor Tests

To assess the new rib design repeatability, the ES-2 fitted with the needle bearing ribs was subjected to sets of three repeat high mass impactor tests at the angle of +20 degrees and two repeats correspondingly at the remaining impact angles of -10, 0, and +10 degrees. The deflections for the upper, middle, and lowers ribs from the repeat tests at +20 degrees are presented in Figures 61-63 and demonstrate good repeatability for the needle bearing rib module design. Similar results were obtained with the two sets of repeat tests at the remaining impact angles.

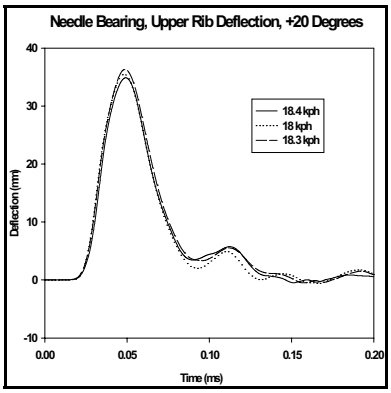

Figure 61.

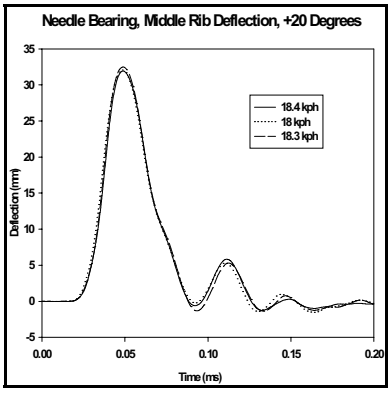

Figure 62.

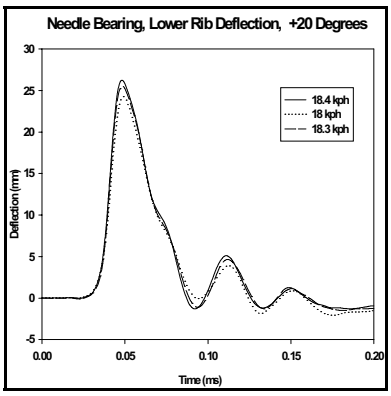

Figure 63.

ES-2 Responses in Sled Tests

To obtain an initial assessment of the overall repeatability of ES-2 dummy, two sets of three sled tests were performed at both the 6.7 m/s padded wall and the 6.7 m/s rigid wall test conditions (Table 7). The arm of the dummy was straight down in these tests.

Table 7.

Test No.	Sled Test	Padding (Kpa)	Dummy Clearance
1, 2, & 3	6.7 m/s padded	103 foam, 4" thick	12"
1, 2, & 3	6.7 m/s rigid	none	12"

The over plot data for the rigid wall repeat tests (Examples in Figures 64-69) show very good repeatability of the ES-2 responses in the three test performed. Relatively good repeatability is seen in the three padded sled tests (Figures 70-74).

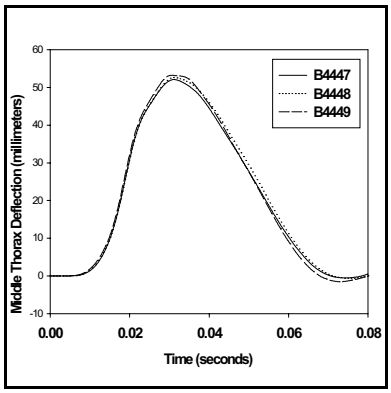

Figure 64. Rigid low speed

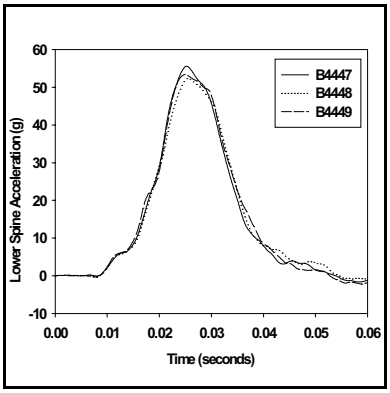

Figure 65. Rigid Low Speed

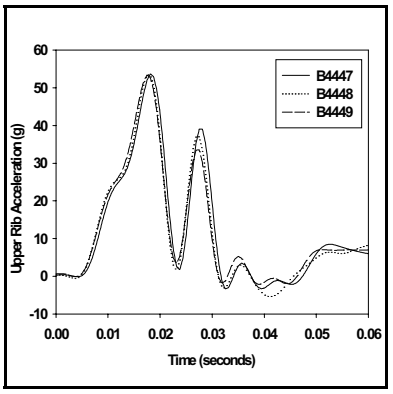

Figure 66 Rigid Low Speed

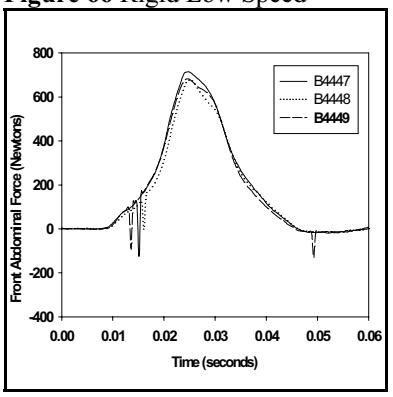

Figure 67. Rigid Low Speed

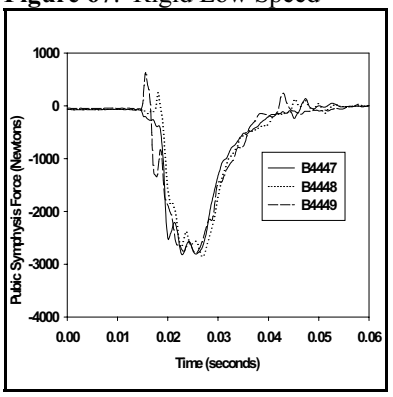

Figure 68. Rigid Low Speed

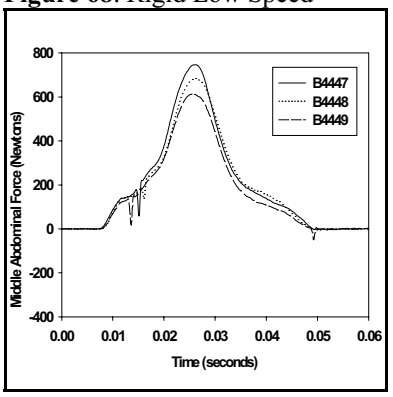

Figure 69. Rigid Low Speed

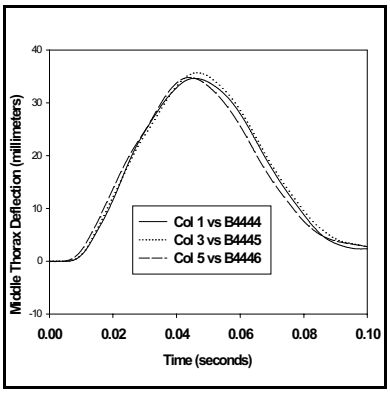

Figure 70. Padded Low Speed

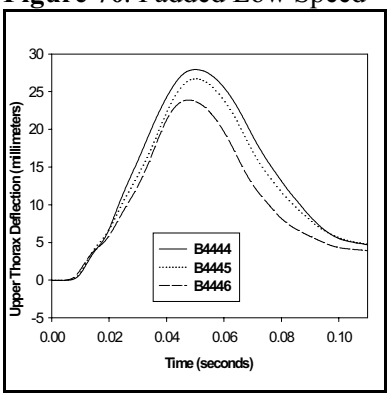

Figure 71. Padded Low Speed

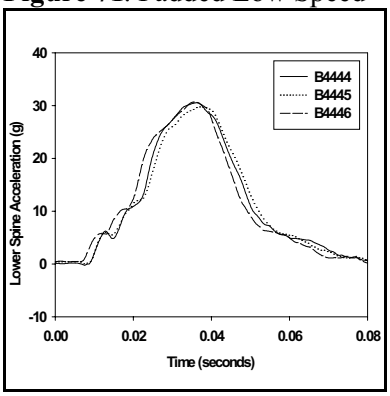

Figure 72. Padded Low Speed

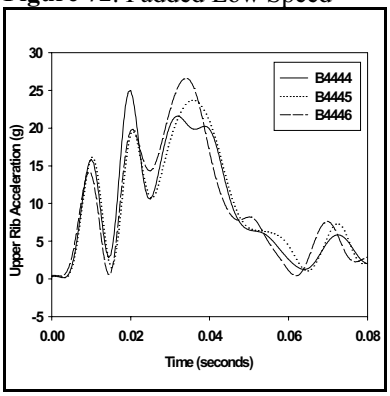

Figure 73. Padded Low Speed

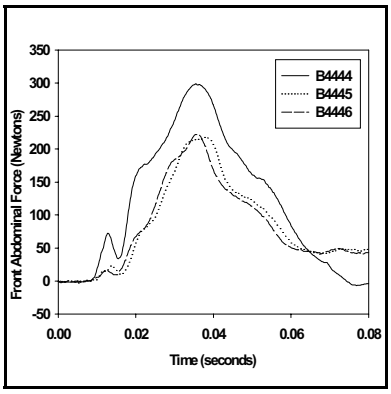

Figure 74. Padded Low Speed

ES-2 Responses in Repeat FMVSS 214 Tests

The two FMVSS 214 tests with the Ford Taurus were intended to provide an initial indication of the repeatability of the ES-2 dummy in the FMVSS 214 test configuration. It is demonstrated in this section that the ES-2 dummies in the two tests were subjected to different loading conditions and, as such, the two tests did not serve as true repeat tests. As shown by the data in Tables A1-A4 (APPENDIX A), the driver peak responses for the shoulder, lower spine (T12), and abdominal forces are considerably higher in Test # 2. The pelvis peak acceleration and pubic symphysis force are slightly higher in Test #2. On the other hand, the peak rib accelerations, ribs deflections, and V*C are considerably higher and occur later in Test #1. With exception of the rib responses, all the driver dummy responses were synchronized in time between the two tests. The dummy responses in Figures 75 and 76 show the later rib acceleration responses relative to the abdomen and public loads in Test #1 in contrast with the more synchronized comparison dummy responses in Test#2.

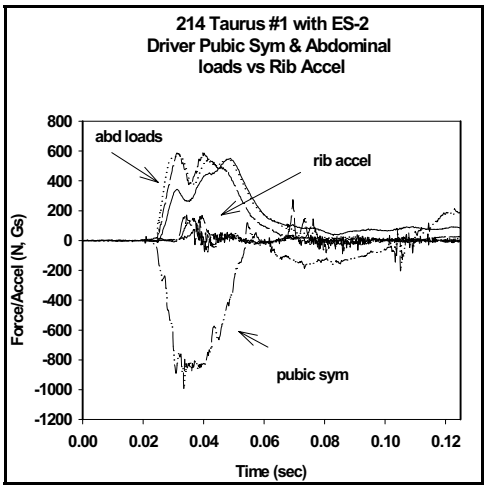

Figure 75.

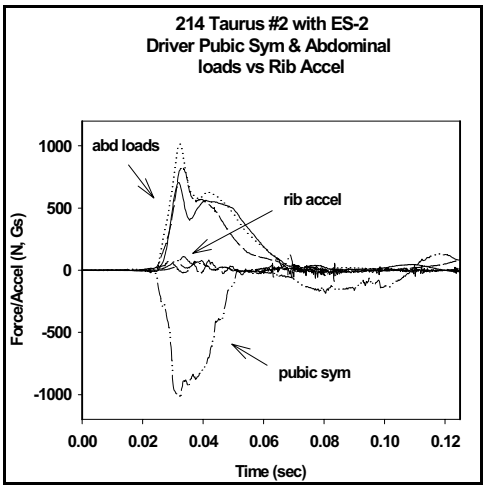

Figure 76.

The Movable Deformable Barrier (MDB) velocity (Figure 77), the vehicle floor pan velocity (Figure 78), and the general test measures such as the impact speeds, impact locations, and the dummy lateral clearances (Table 7), indicate that the general conditions for the two FMVSS 214 tests were very close.

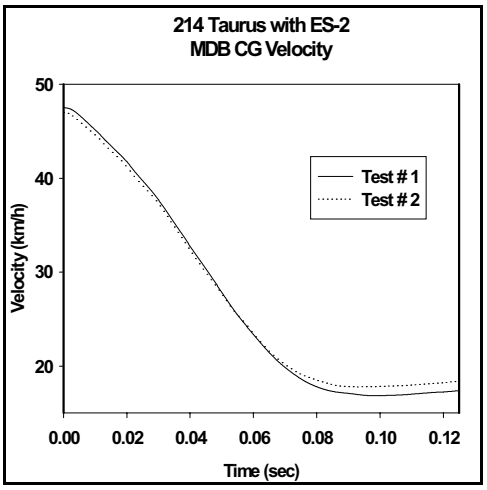

Figure 77.

Comparisons of the vehicle velocities at the left front sill, lower door centerline and the driver seat track (Figures 79-81) indicate that the MDB had less engagement with the sill in Test #2. This coupled with the dummy seated lower in the seat in Test #2 (H-pt from ground in Table 7) would explain the higher loadings experienced by the dummy, especially in the upper body segments. It is worth noting that the 1996 MY Taurus vehicles tested were purchased used and probably were driven by occupants of different stature, which could effect H-pt to ground height of the seated dummy. It is also important to note that bumper section separated from the MDB front face in Test#2 which may account for the difference in MDB to vehicle engagement between the two tests.

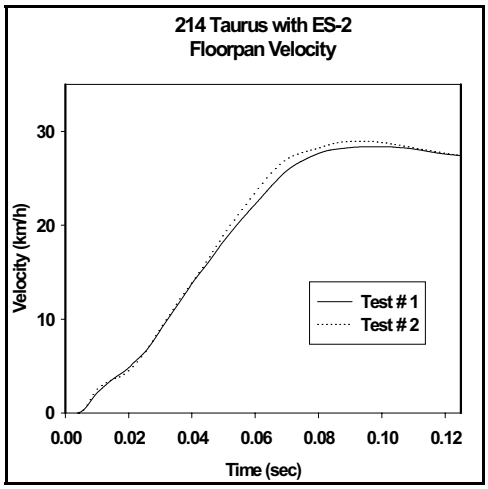

Figure 78.

TABLE 7. FMVSS 214 Test Measures

	TEST #1	**TEST #2**
H-point driver, from front axle (mm)	1253	1258
H-point driver, from ground (mm)	**460**	**434**
Impact point (from striker X-dir) (mm)	3 forward	8 forward
Impact point (from striker Z-dir) (mm)	4 low	0
Arm to door (mm)	115	115
H-point to door (mm)	155	158
Head to roof (mm)	194	195
Head to side (mm)	295	298
Frt seat back crush (mm)	**76**	**39**
Frt seat cushion crush (mm)	61	56
Driver arm angle relative to window sill (°) -from film	**29**	**26**
Vehicle weight (kg)	**1769**	**1775.8**
Impact Speed (km/h)	53.3	52.3

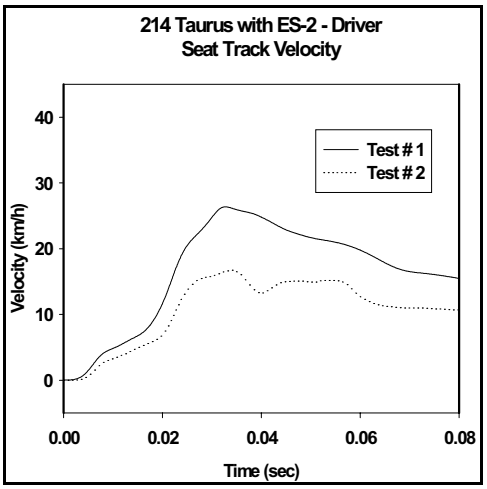

Figure 79.

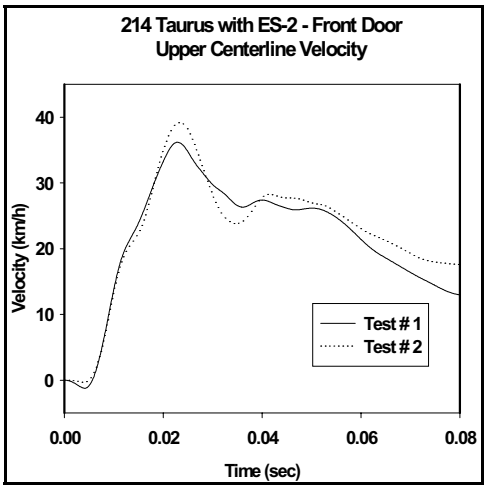

Figure 81.

Reviewing the films from both tests indicated that, initially, the dummy arm in Test #1 was lower, relative to window sill, than in Test #2 (Table 7). The films also indicated that the upper body of the dummy in Test#1 rotated more towards the door. It is presumed that the dummy arm may have further dropped at the time of impact in Test #1 and thus did not shield the dummy's thorax from the door impact. This would result in the delayed but higher rib accelerations seen for the driver dummy in Test#1.

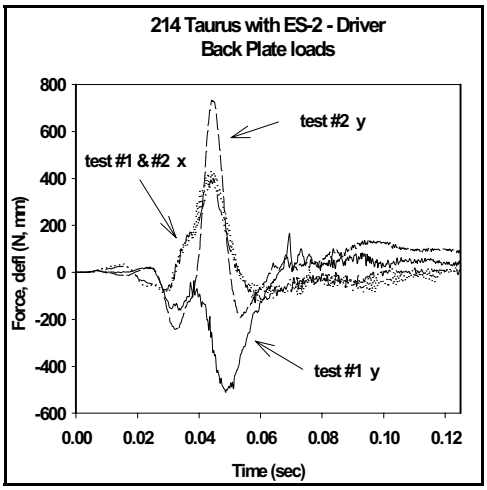

Figure 82.

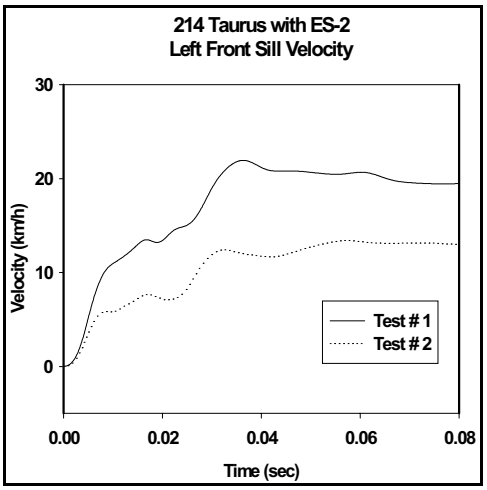

Figure 80.

There is considerably more crush in the driver seat back in Test#1 (Table 7). Examining the back plate loads for both tests (Figure 82) shows a very good match of the loads in the x direction, while the lateral back plates differ considerably. In Test #1, the back plate is pushed to the left, unloads, and then pushed to the left again. In Test #2, the back is first pushed to the left with a lower peak load, unloads, and then is pushed to the right with an increasing load. This, along with the larger crush for the driver seat back suggests that the dummy was pinned in the seat in Test #1 and, as such, would contribute to the higher rib deflections seen in Test#1.

SUMMARY OF FINDINGS

- The side crash problem for recent model year vehicles in the US indicates a relative increase in serious injuries to the head, abdomen, and pelvic body regions and a relative decrease in the proportion of serious thoracic injuries.

- Based on comparison with baseline tests in accordance with the EU 96/27/EC test conditions, the rib deflection flat top response has been reduced in the ES-2 dummy relative to the EUROSID-1.

- Based on the FMVSS 214 and the US Side NCAP tests performed, the following is noted:
  - Rib deflection flat top response was not present in the FMVSS 214 tests but may need to be investigated further in US Side NCAP tests
  - ES-2 back plate loads are very small when compared with other forces acting on the dummy however the significance of these loads on overall dummy responses has not been assessed
  - Knee-to-knee contact in the ES-2 had little or no effect on pubic symphysis loads

- Overall, ES-2 responses showed good repeatability in the limited sled tests
  - ES-2 new rib module design showed good repeatability in component level tests
  - Additional full scale tests are needed to investigate the arm to door interaction and the resulting effect on the rib deflections

FUTURE RESEARCH

Based upon the results from the testing performed with the ES-2 dummy, the following research is planned:

- FMVSS 214 and US Side NCAP tests with current vehicle models, including side air bag equipped models, to provide data on fleet performance with the ES-2.

- Side impact pole tests and FMVSS 214 tests, with a higher and heavier movable deformable barrier, to provide data on ES-2 head and neck responses and investigate shoulder interaction.

- Additional sled tests to provide a more complete assessment of biofidelity.

- Component and sled tests to assess back plate interaction with the seat back.

- Development and application of injury criteria for the ES-2 dummy.

REFERENCES

1. National Highway Traffic Safety Administration; NHTSA Plan for Achieving Harmonization of the U.S. and European Side Impact Standards, Report to Congress, April 1997.
2. Samaha, R. R; Molino, L. N; Maltese, M. R., "Comparative Performance Testing of Passenger Cars Relative to FMVSS 214 and the EU 96/EC/27 Side Impact Regulations: Phase I", Paper 98-S8-O-08, 16th Annual ESV Conference, Windsor, Canada, 1998.
3. Maltese, Samaha, Eppinger, Strassburg, "Response of the Eurosid-1 Thorax to Lateral Impact", SAE Paper No. 99010709.
4. Federal Register Vol. 65, No. 101, May 24, 2000, p. 33508, Dept. of Transportation, NHTSA, 49 CFR Part 571, ACTION: Grant in part, denial in part of petition for rulemaking.
5. Van Ratingen, Waagmeester, Twist, and Wisman, "Harmonizing the European Side Impact Dummy", JSAE 2000, SAE Paper No. 20005318.
6. Waagmeester, Twist, Philippens, Van Ratingen, "Task 4.2: Status of Side Impact Development in Europe-Development of EUROSID-2", SID-2000 Report, Brite-Euram Project,CT98 0632, June 2000.
7.Kuppa, Eppinger, Maltese, Naik, Pintar, Yoganandan, Saul, McFadden, Assessment of Thoracic Injury Criteria for Side Impact, IRCOBI, 2000.
8. ES-2 Prototype User Manual, TNO Automotive, Crash Safety Centre, March 2000.
9. Morgan, R.M., Marcus, J.J., Eppinger, R.H., "Side Impact - The Biofidelity of NHTSA's Proposed ATD and Efficacy of TTI", SAE Paper No. 861877.

ACKNOWLEDGMENTS

The authors would like to acknowledge the contribution of Gary Strassburg, Dave Kovloski, Tim Macknay, Chris Novak, John Wistert of MGA Research, Marie Hansen of Capitol Consulting, Dr. Tom Trella of VNTSC/RSPA, Ryan Park of Conrad Technologies, and Salwa Radwan for their contributions in performing the testing and analyses presented in this paper.

APPENDIX A

Table A1. Full Scale Driver Test Results - Rib Deflections and V*C

vehicle/test	RDC	up rib defl CFC 180	mid rib defl CFC 180	low rib defl CFC 180	V*C	V*C upp rib	V*C mid rib	V*C low rib
	(mm)	(mm)	(mm)	(mm)				
EU Taurus/EUROSID-1	40	30	38	40	0.94	0.67	0.94	0.94
EU Taurus/ES-2	51	38	47	51	1.43	0.75	1.26	1.43
214 Taurus #1/ES-2	40	39	40	37	0.65	0.65	0.58	0.59
214 Taurus #2/ES-2	35	35	33	24	0.36	0.36	0.34	0.18
EU Metro/EUROSID-1	44	44	38	28	0.65	0.65	0.51	0.35
EU Metro/ES-2	48	48	44	34	1.12	1.12	1.00	0.80
NCAP Cavalier/ES-2	51	51	47	31	1.05	1.05	1.05	0.77
NCAP Grand Am/ES-2	51	51	29	16	0.99	0.99	0.55	0.27

Table A2. Full Scale Driver Test Results - Shoulder, Abdomen, Lower Spine, Pubic Symphysis, and Left Femur Loads

vehicle/test	sh y	sh z	back pl x	back pl y	APF	T12 y	Pubic Sym	lft fem y	lft fem l z
	(N)	(N)	CFC 600 (N)	CFC 600 (N)	CFC 600 (N)	CFC 600 (N)	CFC 600 (N)	CFC 600 (N)	CFC 600 (N)
EU Taurus/EUROSID-1					1131		-2196		
EU Taurus/ES-2	309	543	179	-316	1740	1770	-917	1267	852
214 Taurus #1/ES-2	518	1288	433	-511	1551	2194	-927	1407	-828
214 Taurus #2/ES-2	771	1412	399	734	2513	2618	-1020	1409	-840
EU Metro/EUROSID-1					1518		-4158		
EU Metro/ES-2	824	735	241	-450	1344	1369	-3512	1706	-1281
NCAP Cavalier/ES-2	991	1275	1168	889	2536	3041	-1620	-2558	1805
NCAP Grand Am/ES-2	4091	600	265	-658	2587	3654	-1786	-1560	1309

Table A3. Full Scale Driver Test Results- Rib, Pelvis, and Spinal Accelerations

vehicle/test	TTI	up rib	mid rib	lower rib	lower spine	upp spine	Pelvis
		FIR100 (G)	FIR 100 (G)	FIR100 (G)	FIR100 (G)	CFC 180 (G)	FIR100 (G)
EU Taurus/EUROSID-1	125	154	166	150	86	101	63
EU Taurus/ES-2	111	99	163	158	59	46	69
214 Taurus #1/ES-2	93	131	131	134	52	56	72
214 Taurus #2/ES-2	76	99	72	74	54	54	80
EU Metro/EUROSID-1	92	96	118	103	65	59	71
EU Metro/ES-2	106	144	130	137	68	55	72
NCAP Cavalier/ES-2	137	144	159	174	100	92	121
NCAP Grand Am/ES-2	112	156	148	147	69	80	102

Table A4. Full Scale Driver Test Results- HIC and HPC results

vehicle/test	HIC 36	t1	t2	HPC	tc1	tc2
		(ms)	(ms)		(ms)	(ms)
EU Taurus/EUROSID-1	67	48	84	67	116	146
EU Taurus/ES-2	106	57	93	nc		
214 Taurus #1/ES-2	294	53	65	nc		
214 Taurus #2/ES-2	150	53	89	nc		
EU Metro/EUROSID-1	97	38	64	nc		
EU Metro/ES-2	184	34	64	177	32	66
NCAP Cavalier/ES-2	592	42	62	nc		
NCAP Grand Am/ES-2	546	45	81	nc		

APPENDIX B
Analysis of Side Impact Cadaver Sled Tests

Introduction

A total of Forty-five side impact PMHS (post-mortem human subject) sled tests were conducted at the Medical College of Wisconsin and the NHTSA Vehicle Research and Test Center in cooperation with the Ohio State University [1]. Tests were conducted at a variety of speeds, with padding and rigid load surfaces, and a variety of door geometry conditions.

Methods

Unembalmed fresh or fresh frozen cadaver subjects were screened for HIV and Hepatitis B and C by drawing blood prior to use. Radiographic examination of all body regions and patient histories were examined to exclude specimens with bone disease and metastatic cancer; subjects' deaths were primarily attributed to cardiopulmonary disease. The cadaver surrogates were cleaned and dressed with a tight fitting leotard and a head/face mask to insure confidentiality.

Test subjects were instrumented with either two or three chestbands [2]. The upper chestband was placed just below the axilla, the middle band at the base of the sternum, and the lower band at the mid-abdomen. Accelerometers were attached to bone at T1-T4, T12, left and right lateral ribs four and eight, upper sternum, and sacrum. The vascular systems of the MCW test subjects were pressurized, while the VRTC test subjects were not.

The sled apparatus was of the Heidelberg [3] design and was propelled on a rebound sled at MCW, and an HyGe acceleration track at VRTC. The test subjects were seated on the bench of the side impact sled roughly 1 meter from the load wall (Figure 1).

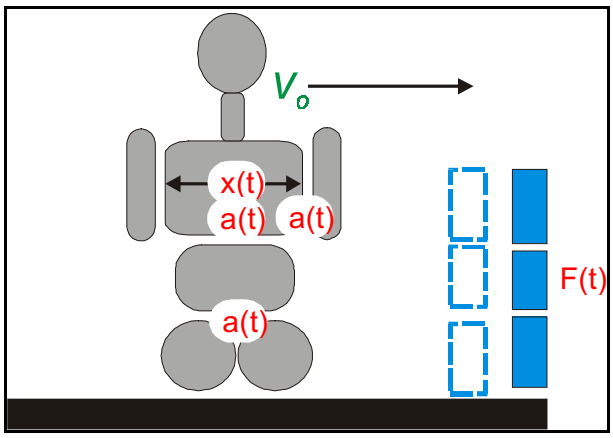

Figure 1 - Schematic of sled test system, showing instrumented occupant with an initial velocity closing on impact with an instrumented load wall. Dotted boxes show thoracic, abdominal and pelvic offset load wall options.

In the test, a force F is applied to the sled to change its velocity, and thus the unrestrained test subject begins to slide relative to the sled towards the load wall. After the sled reaches the prescribed velocity, the force F is removed and the occupant contacts the load wall. The sled continues to move along the track at near-constant velocity during

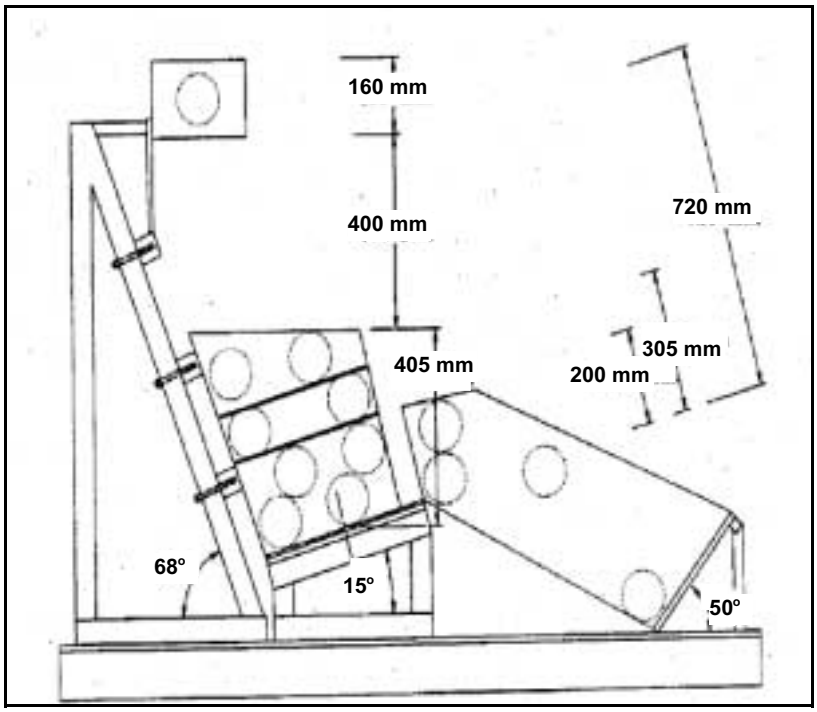

Figure 2 - Cross-section view of NHTSA/MCW sled buck.

occupant interaction with the load wall, before the sled is gradually slowed by a braking system. The load wall is divided into four sections, one each to contact the thorax, abdomen, pelvis, and legs (Figure 2). Force transducers between the sled and the load plates measure occupant loads from each body region.

Test Conditions - The change in velocity of the sled was either 6.7 or 8.9 m/s (±0.3 m/s). The load wall was either rigid or padded with 10 cm of LC200 padding (compressive stiffness = 103 kPa). The geometry of the load wall was also a variable, as the load plates were either fixed in the same plane, or the thoracic, abdominal or pelvic plates were each, one at a time per test, offset towards the occupant by 12 cm. In the flat wall and pelvic offset tests, the cadaver was seated with its arms down, such that the arm was interposed between the thorax and load wall. In the thoracic and abdominal offset tests, the arms were raised to expose the thorax and abdomen directly to impact from the load wall. High speed 16 mm film and digital video cameras recorded the side impact event. There was one overhead view, one onboard anterior view and two off board posterior views. Five tests were excluded from the analysis due to data acquisition system failures, short stature subjects, or test speeds falling outside the speed categories of 6.7 and 8.9 m/s (±0.3 m/s).

Signal Analysis - All acceleration and force signals were filtered using a CFC 180 Butterworth filter and subsampled at 0.001 second time step. Chestband gauge signals were filtered at CFC 600, and torso deformation contours were calculated at 0.001 second intervals.

Full Chest Deflection - The following process was used to determine the full chest deflection:
Six locations on each deformation contour were selected for development of torso deflections (Figure 3). Starting at the spine and following the contour in a clockwise direction, locations were marked at 20%, 25%, 30%, 70%, 75%, and 80% of the contour circumference.

The linear distance between location pairs 30% and 70%, 25% and 75%, and 20% and 80% was calculated, and then averaged to determine the mean torso deflection. The above steps were repeated for subsequent time steps to create the full deflection time history for a particular Chestband location.

Also calculated was the half-chest deflection, which was determined as follows: Three locations on each deformation contour were selected for development of Chestband deflections (Figure 3). Starting at the spine and following the contour in a clockwise direction, locations were marked at 20%, 25%, and 30% of the contour circumference. A line was constructed between the sternum and spine locations on the band, and the points found in the previous step were projected in the lateral direction onto the sternum-spine line. The distance between each point on the left side and its projected partner. Three distances were found per Chestband and averaged to find the mean deflection. This was repeated for subsequent time steps to create the half deflection time history for a particular Chestband location.

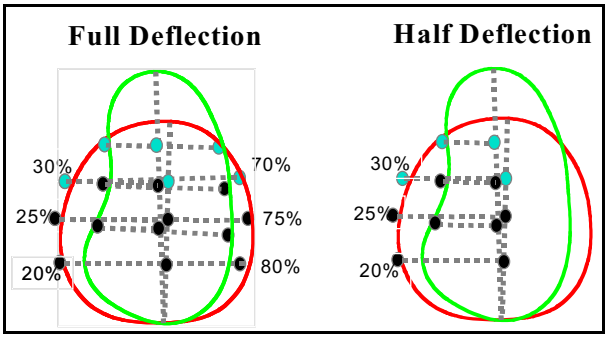

Figure 3. Diagram of chest deflection calculation methods. Full chest deflection is calculated using points spanning the entire width of the Chestband, while half chest deflection calculates the length of a line between a point on the left side of the contour, to a point on the sternum to spine line, at the same distance along the anterior-posterior coordinate axis.

Newtonian scaling[4] was employed to normalize the data to a 50th percentile male. Assuming that modulus of elasticity and density are equal from subject to subject, mass-based scaling was used on all force, deflection and acceleration signals, according to:

Acceleration:	$A_s = \lambda_m^{-1/3} A_i$
Length:	$L_s = \lambda_m^{1/3} L_i$
Force:	$F_s = \lambda_m^{2/3} F_i$
Time:	$T_s = \lambda_m^{1/3} T_i$

where s is the subscript for scaled data, i is the subscript for i-th test subject, and

$$\lambda_m = 75/m_i$$

where m is the subject mass in kilograms.

Corridor Calculation - For flat wall tests, the start of the impact event was determined by the initiation of arm contact on the thoracic load plate. In offset tests, the start of the impact event was timed with first contact on the offset load plate. The tests were grouped by test condition - rigid 8.9 m/s flat wall, padded 8.9 m/s flat wall , rigid 6.7 m/s flat wall, padded 6.7 m/s flat wall, rigid 6.7 m/s abdominal offset test (arm up) and padded 6.7 m/s pelvis

offset test. Signals common to all tests were then processed to calculate the standard deviation for each point in time according to,

$$S_t = \left[\sum_{i=1}^{n} \frac{(x_{i,t} - \bar{x}_t)^2}{n-1} \right]^{1/2} \qquad t = 1 \ldots m$$

where

$\bar{x}_t = \sum_{i=1}^{n} \frac{x_{i,t}}{n}$ is the mean

$x_{i,t}$ is the value of the ith measurement curve at time step t

n is the total number of measurement curves

m is the total number of time steps

Upper and lower corridors were determined, respectively, by adding and subtracting standard deviation time histories from the mean time history.

APPENDIX B REFERENCES

1. Pintar FA, Yoganandan N, Hines MH, Maltese MR, McFadden J, Saul R, Eppinger R, Khaewpong N, Kleinberger M, "Chestband Analysis of Human Tolerance to Side Impact", Proceedings of the 41st Stapp Car Crash Conference, Society of Automotive Engineers, 1997.

2. Eppinger RH, "On The Development Of A Deformation Measurement system And Its Application Toward Developing Mechanically Based Injury Indices." Proceedings of the 33rd Stapp Car Crash Conference, Society of Automotive Engineers, 1978.

3. Kallieris D, Mattern R, Schmidt G Eppinger RH, "Quantification of Side Impact Responses and Injuries", Proceedings of the 25th Stapp Car Crash Conference, Society of Automotive Engineers, 1981.

4. Eppinger RH, Marcus JH, Morgan RM, "Development of Dummy and Injury Index for NHTSA's Thoracic Side Impact Protection Research Program", Proc. 28th Stapp Car Crash Conf, Society of Automotive Engineers, Inc., 1984:983-1011.